Probing Mechanical Activation of Covalent Chemistry in Crosslinked Polymer Gels

by

Yifei Wang

Department of Chemistry
Duke University

Date:_____

Approved:

_____
Stephen L. Craig, Supervisor

_____
Michael J. Therien

_____
Patrick Charbonneau

Thesis submitted in partial fulfillment of
the requirements for the degree of Master of Science in the Department of
Chemistry in the Graduate School
of Duke University

2013

ABSTRACT

Probing Mechanical Activation of Covalent Chemistry in Crosslinked Polymer Gels

by

Yifei Wang

Department of Chemistry
Duke University

Date:_____

Approved:

_____
Stephen L. Craig, Supervisor

_____
Michael J. Therien

_____
Patrick Charbonneau

An abstract of a thesis submitted in partial
fulfillment of the requirements for the degree
of Master of Science in the Department of
Chemistry in the Graduate School of
Duke University

2013

# Abstract

Toughness, the measure of how much energy a material can absorb before rupture, is an important property of materials. It has been demonstrated that the toughness of a single polymer chain of *gem*-dihalocyclopropane (*g*DHC) functionalized polybutadiene (PB) is increased dramatically over PB alone, due to the mechanically triggered electrocyclic ring opening reaction of *g*DHC into 2,3-dibromoalkenes. This thesis explores whether this molecular mechanical property can also be manifested in bulk material properties. Crosslinked *gem*-dichlorocyclopropane (*g*DCC) embedded PB polymers were swollen in various solvents, and the resulting gels were mechanically deformed under tensile stress. Young's modulus and fracture toughness were compared among PBs with *g*DCC incorporated in the backbones and/or crosslinking positions. The results showed that the incorporation of *g*DCC does not measurably increase the fracture toughness of the crosslinked polymer gels. Neither NMR nor FT-IR characterization of the post-test samples revealed detectable activation of the *g*DCC in the crosslinked PB. Further experiments will be focused on optimizing the polymer structure and testing methods to more effectively transfer the macroscopic force to the mechanophore in the material and continuing exploring the correlation between molecular responses and changes in macroscopic properties.

# Contents

# List of Tables

# List of Figures

# List of Scheme

# Acknowledgments

I would like to express the deepest appreciation to my committee chair, Professor Stephen L. Craig, who has the attitude and the substance of a genius: he continually and convincingly conveyed a spirit of adventure in regard of research and scholarship. Without his guidance and persistent help this thesis would not have been possible.

I would like to thank my committee members, Professor Michael J. Therien and Professor Patrick Charbonneau, who gave me valuable scientific advice on the content of this thesis. I would like to thank Professor Xuanhe Zhao, for his scientific advice on the mechanical testing experiments.

In addition, a thank you to all the colleagues in the Craig lab: Zach Kean, Junpeng Wang, Bobin Lee, Zhenbin Niu, Jennifer Hawk, Ashley Black, Gregory Gossweiler, for your constant and kind help during this two year experience. Without you I could never have survived graduate school. Thank you for making this experience full of fun and happiness.

I also thank my friends (too many to list here but you know who you are!) for providing support and friendship that I needed.

I especially thank my mom and dad for providing unconditional love and care for me. I would never have made it this far without them. I know I always have my family to count on when times are rough.

# I. Introduction

Polymer materials, ranging from synthetic plastics to biopolymers, play an essential role in everyday life because of their excellent characteristics: good moldability, good corrosion resistance, low production cost, etc... Some characteristics, however, such as low tensile strength and/or poor temperature resistance have limited their applications. As a result, how to extend the lifetime of the material and improve its mechanical properties has become an important topic both in chemistry and material science. Mechanical properties of polymers are a function of their structure, including short- and long-range atomic structure and structure on higher (supramolecular and microscopic) levels.[1] Structures on different levels respond to mechanical stimuli via different mechanisms, and, as a result, the stimuli affect the mechanical properties differently.[2] Particular to our interest are the mechanochemical changes on an atomistic level, where changes in chemical bonding and conformation occur.

Much work has been done in the past century in understanding the molecular response to mechanical stimuli. In 1940, Kauzmann and Eyring established the activated-rate theory that firstly built up the relationship between mechanical force and chemical changes on the molecular level.[3] Their theory was later extended by Bell.[4] Briefly, if as the chemical potential energy increases on going from the ground state to the transition state during the reaction, a coupled mechanical potential energy decreases,

then the net activation energy of the coupled system can be lowered by applying a force towards the direction from the ground state to the transition state.

Recent work has demonstrated that certain chemical bonds are more chemical reactive than others under mechanical force,[5,6,7] which leads to a new direction in the design of organic compounds – incorporating molecules into specific positions in the polymer backbones to trigger targeted cleavage or rearrangement of chemical bonds in the polymers when force is applied. These mechanically active molecules are called "mechanophores." Examples include the stress-induced ring opening of spiropyran to a purple-colored merocyanine that allows direct and local visualization of the mechanochemical reactions in the solid state;[7] the ultrasound-induced electrocyclic ring opening of benzocyclobutene derivatives, which shows that applying a mechanical force can fundamentally alter the potential energy surface of the reaction and provide access to the thermally forbidden products;[6] the cycloreversion of cyclobutane[8] and mechanically responsive materials based on Diels-Alder/retro-Diels-Alder reactions,[9,10] and others.[11,12,13] Almost all these approaches, however, focus on investigating the relationship between the molecular mechanical activation and the macroscopic stimuli. This thesis investigates whether mechanophore activity can lead to enhanced toughness in macroscopic materials.

Our hypothesis comes from single molecular force spectroscopy (SMFS) studies of *gem*-dibromocyclopropane (*g*DBC) mechanophores that were incorporated into

polybutadiene (PB).[14] It was shown that, under sufficient tension, all of the *g*DBC mechanophores in a single *g*DBC-PB copolymer chain undergo an electrocyclic ring opening reaction to the corresponding 2,3-dibromoalkene, leading to a *ca.* 28% increase in the contour length of the polymer. Because the extension occurs at high force (*ca.* 1 nN on timescales of seconds), this transformation leads to a substantial increase in the toughness of the single chain prior to failure (Figure **1**). Similar results have been observed with other gem-dihalocyclopropanes (*g*DHCs).[15]

The result exemplifies one attractive, but speculative, strategy for self-toughening material design, and we wondered about the consequences of such activity on bulk material properties. The advantage of the *gem*-dihalocyclopropane system in probing this relationship is twofold. First, the mechanophores can be incorporated into the polymer backbones in large amounts through a one-step reaction. Second, when the *g*DHC is embedded in the polymer backbone, the electrocyclic ring opening to the corresponding 2,3-dihaloalkene is well coupled with mechanical force. The reaction is irreversible, and the products can be quantified spectroscopically.[16] Besides the result from SMFS, we have also demonstrated that the electrocyclic ring opening reactions happen to *gem*-dichlorocyclopropane (*g*DCC), *g*DBC and *gem*-bromochlorocyclopropane (*g*BCC) under different mechanical stimuli. In solution, hundreds of incorporated *g*DCC rings in the polybutadiene polymer backbones open when coupled to ultrasound-generated elongational shear flows.[17] In the bulk, *g*DHC rings were also activated under

extrusion and uniaxial compression.[16, 18] Despite this progress, however, the *g*DHC mechanophore in the linear polybutadiene polymer has never shown activation under tensile deformation in the solid state.[16] One hypothesis is the low probability of sufficient shear stress transfer from the macroscopic force to the specific chemical bonds in the polymer backbones during uniaxial tension, compared to compression and extrusion. During tensile deformation the stress is unevenly distributed in the material, and, we hypothesize, material rupture occurs mainly through disentanglement of the polymer chains, prior to mechanical activation. How changes in the structure of the bulk material influence the transfer of stress to the mechanophores, potentially leading to a toughness increase as observed in SMFS, remains unsolved.

We therefore set out to explore the macroscopic mechanical properties of *g*DHC-incorporated polymeric materials, in an effort to determine whether the self-toughening property of a single polymer chain can be manifested in the bulk material, and to characterize how much activation of the mechanophores in the solid state can be achieved under mechanical loading. The focus of our study is a family of crosslinked polymer gels, and the overarching goal of this project is to elicit structure-activity relationships with respect to mechanochemical activation, with the aim of facilitating the rational design of self-strengthening or self-toughening polymeric materials. The methodology will allow us to address the critical contributions of a very specific

molecular process to material responses, potentially leading to rules for transformative material design.

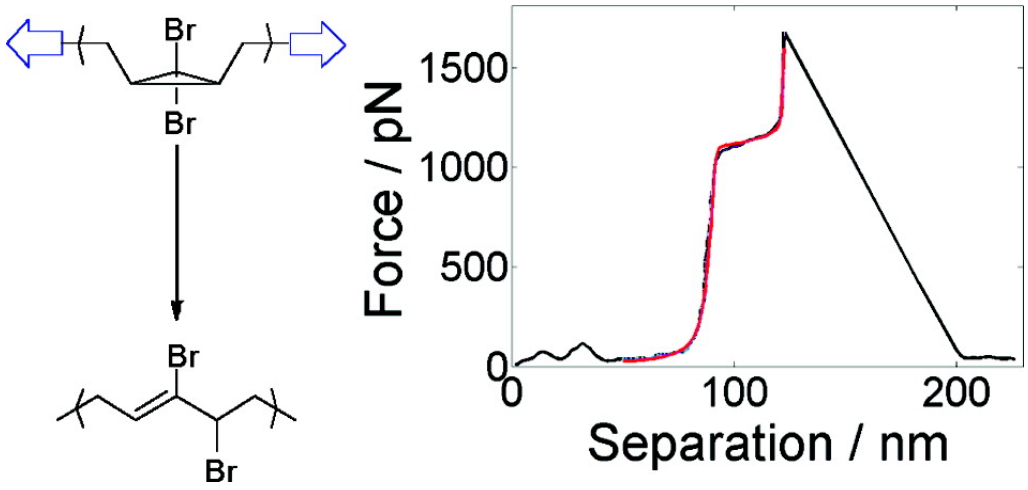


**Figure 1: Single molecular force spectroscopy was used to monitor the electrocyclic ring opening of *gem*-dibromocyclopropane (*g*DBC).[14] On the left, the contour length of the polymer chain increases due to the ring opening of the dibromocyclopropane. On the right is the force versus extension curve. The plateau indicates the stress relief caused by the ring opening of the dibromocyclopropane.**

# II. Methods and Results

## *1. Reagents and Synthesis*

### 1.1 Monomers and Crosslinkers

For preliminary studies, the *g*DCC-functionalized monomer **1a** was synthesized by reacting (1*Z*,5*Z*)-cycloocta-1,5-diene with chloroform.[17] The *g*DCC-functionalized crosslinker **2a** was synthesized by reacting **1a** with potassium permanganate[19] followed by esterification with **1c**.[20] The control crosslinkers **2b** and **2c** were synthesized by reacting **1c** with glutaric acid and octanedioic acid, respectively (**Scheme 1**).

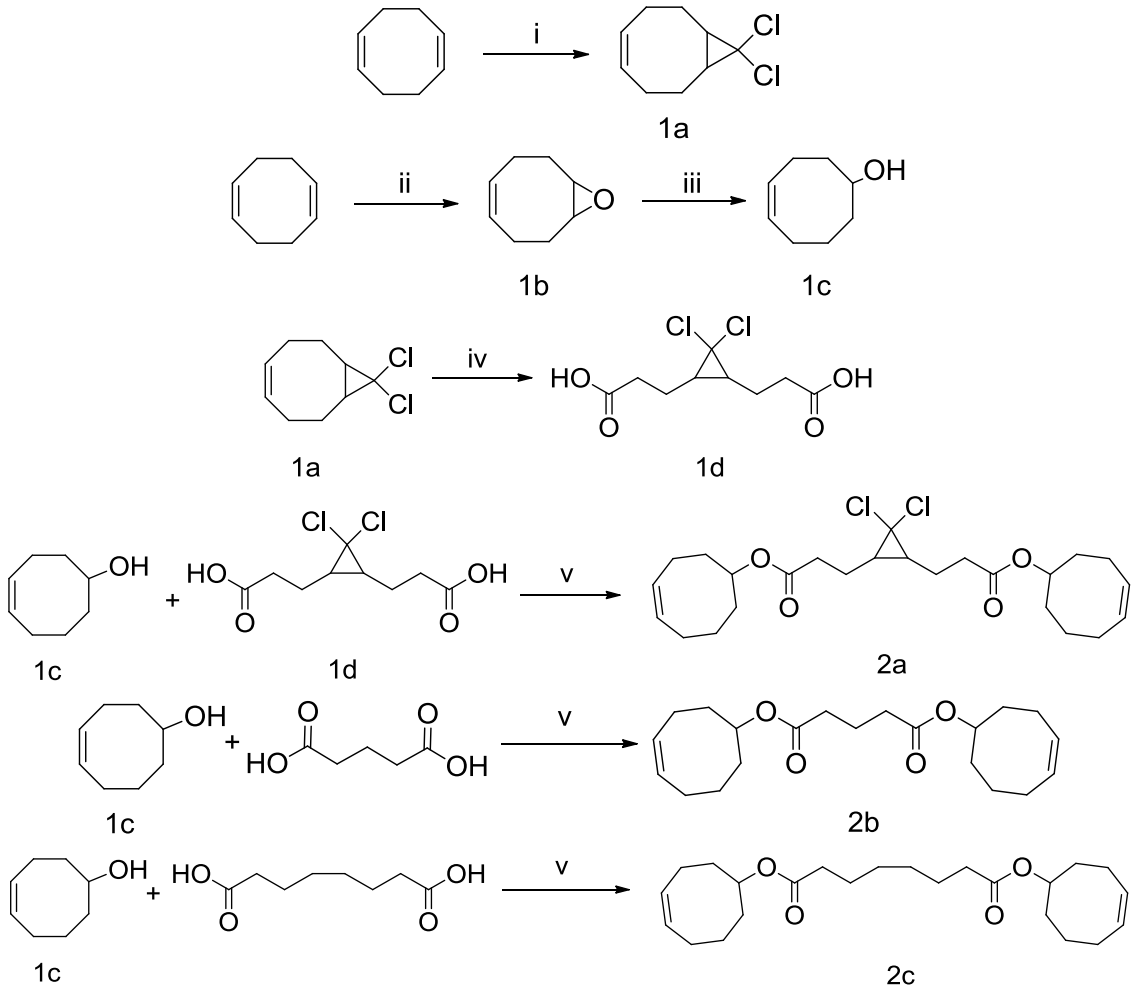


**Scheme 1: Synthesis of *g*DCC functionalized monomer 1a and crosslinkers 2a, 2b and 2c;**

**i. CTAB, NaOH, $CH_2Cl_2$, $CHCl_3$, room temperature, 24 h, $N_2$;[17]**

**ii. *m*CPBA, $CHCl_3$, room temperature, 12 h, $N_2$;[21]**

**iii. LAH, THF, room temperature, 6 h, $N_2$;[21]**

**iv. $KMnO_4$, $NaHCO_3$, acetone, room temperature, 48 h, $N_2$;[19]**

**v. DIC, DMAP, THF, room temperature,24 h, $N_2$.[20]**

## 1.2 Crosslinked Polymer

Crosslinked polybutadiene polymers **3a** to **3e** with *g*DCC embedded in the backbones were synthesized through ring opening metathesis polymerization (ROMP) reaction with different ratios of (1*Z*,5*Z*)-cycloocta-1,5-diene, **1a**, and **2b**. The crosslinked polymers **4a** and **4c** with *g*DCC incorporated in the crosslinking position were synthesized through ROMP reaction with (1*Z*,5*Z*)-cycloocta-1,5-diene and the *g*DCC-functionalized crosslinker **2a**. The control polymers were synthesized similarly, as shown in **Scheme 2**.

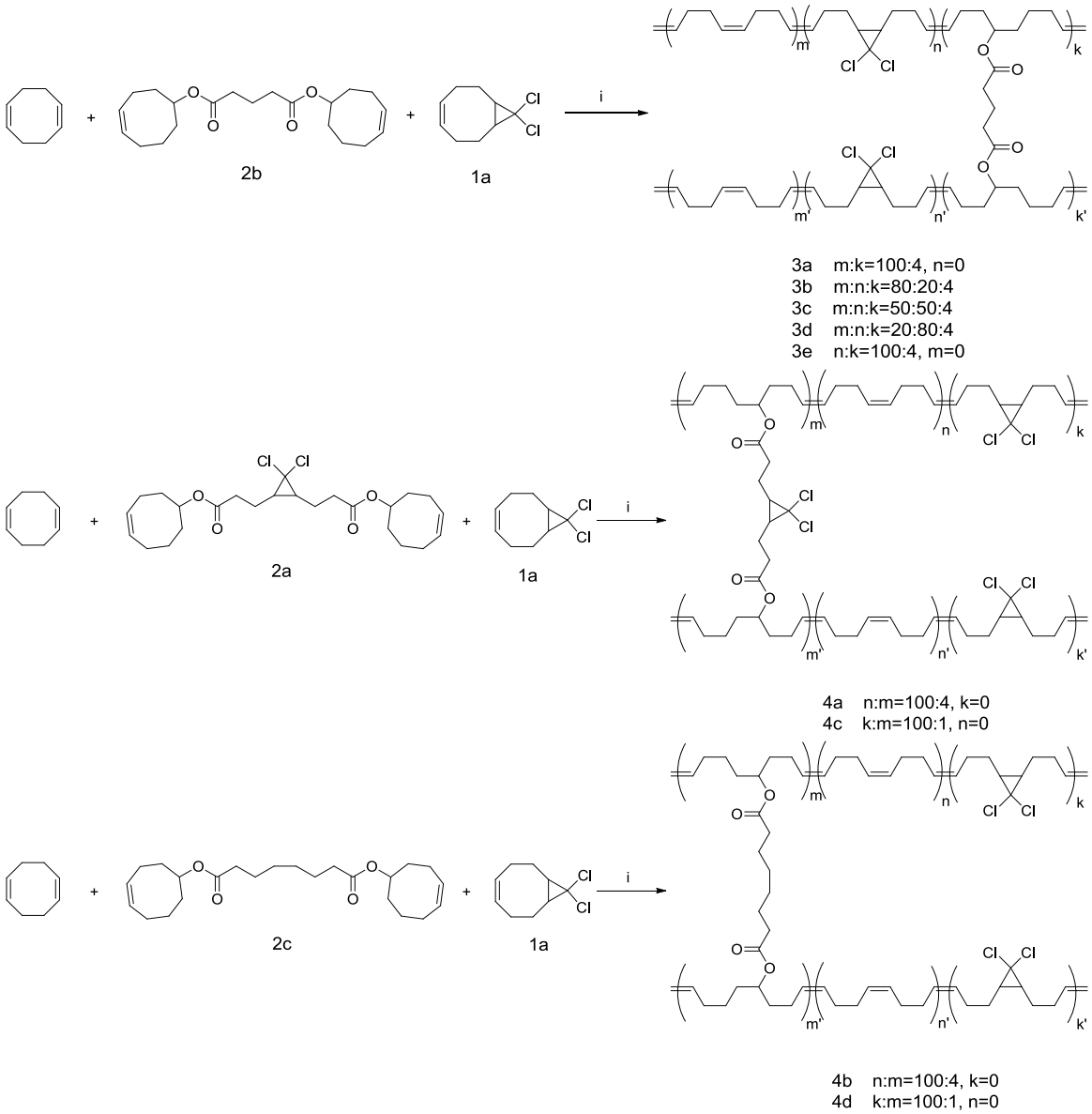


**Scheme 2: Synthesis of crosslinked, *g*DCC-embedded polybutadiene polymer 3a-e and 4a-d with different percentages of *g*DCC. The molar ratio of crosslinker to monomer was kept constant 4:100 (and 1:100 for 4a and 4c for cyclic tensile testing).**

**i. Grubbs 2nd generation catalyst, DCE, BHT, 70 °C, 3h.**

## 2. Swelling Ratio Investigation

The swelling ratio (SR) is here defined as the ratio between the volume of the swollen polymer and the volume of the dry polymer.

$$\text{SR} = \frac{V\ swollen}{V\ dry} \quad (1)$$

An ideal swelling solvent should have low vapor pressure, which minimizes solvent evaporation during tensile testing, and be a good solvent for the polymer, which leads to extensive swelling and minimizes polymer-polymer interactions that vary from one system to another. In order to investigate the effect of the mechanophore activation on the mechanical properties, it is important to maintain a constant SR within the polymer series, so that if there is any difference in properties between the target polymers and the control polymers, it will likely reflect mechanophore activations that happen within the network.

Two methods were used to quantify the SRs of the polymers. First, the swollen polymers were immersed in deionized water to acquire the volume change by solvent displacement before and after swelling. The SR results were not consistent due to the limitation of the container precision. Second, change in film length was measured in one dimension, and the results were cubed to acquire the SR. The method is reasonable since the swelling process is isotropic, the extension change should be the same in all directions as long as the polymer is synthesized uniformly. The SR results were more

consistent compared to those from the first method, and they were adopted for the following solvent investigation.

Different solvents were examined: dichloromethane ($CH_2Cl_2$), chloroform ($CHCl_3$), 1,2-dichlorobenzene (DCB), 1,2,4-trichlorobenzene (TCB), dimethyl sulfoxide (DMSO), dimethyl formamide (DMF), hexadecane, 2-pyrrolidone and decalin, which are chosen based on their dielectric constant and vapor pressures. The results are shown in Table **1**. For the same polymer, different solvents give different SRs. Of all the solvents tested, $CHCl_3$ produced the largest SR, while DMSO yielded the lowest. We settled on TCB and hexadecane because they both have low vapor pressures and have significantly different SRs for the material.

Since the polymers with different percentages of *g*DCC have different SRs in any given solvent and swelling influences mechanical properties, it is hard to compare modulus and toughness trends across the series in a single solvent. As a result, it is essential to eliminate the effects caused by the different swelling extent. As can be seen in Figure **2**, SR increases when more *g*DCCs are incorporated in the backbones and TCB is the solvent. Also by using a mixture of a good and a poor solvent (*e.g.* TCB and hexadecane), the SRs increase for the same polymer as the good solvent percentage increases.

After numerous trials, the SRs for the polymer series with different percentages of *g*DCC in the backbones were unified to *ca.* 3.0 with mixed solvents of TCB and

hexadecane, and 3.0 for polymer series with mechanophore incorporated in the crosslinking position for the fracture toughness test, as shown in Figure **3** and Table **2**. The SR for the polymer series with *g*DCC incorporated in the backbones and in the crosslinking positions are unified to *ca.* 4.0 and 6.5, respectively, for hysteresis testing, as shown in Table **3**.

**Table 1: Swelling Ratio (SR) of PB gels with *g*DCC in the backbones. DCB, decalin and TCB were used for tensile tests. Other solvents were used to test the swelling range.**

| Swelling Solvent | Vapor pressure (mm Hg) | Dielectric constant (ε) | SR | |
|---|---|---|---|---|
| | | | PB | 100% *g*DCC |
| DCB | 1.2 | 9.93 | 3.2 | 3.8 |
| decalin | 1.2 | 2.16 | 2.6 | 3.5 |
| TCB | 0.39 | 2.24 | 3.0 | 3.2 |
| hexadecane | 0.005 | 2.08 | 1.5 | 1.2 |
| 2-pyrrolidone | 0.01 | 27.37 | 1.1 | 1.1 |
| DMSO | 0.42 | 46.68 | 1.1 | 1.0 |
| DMF | 2.7 | 36.71 | 1.2 | 1.3 |
| $CHCl_3$ | 160 | 4.81 | 3.6 | 3.8 |

a)

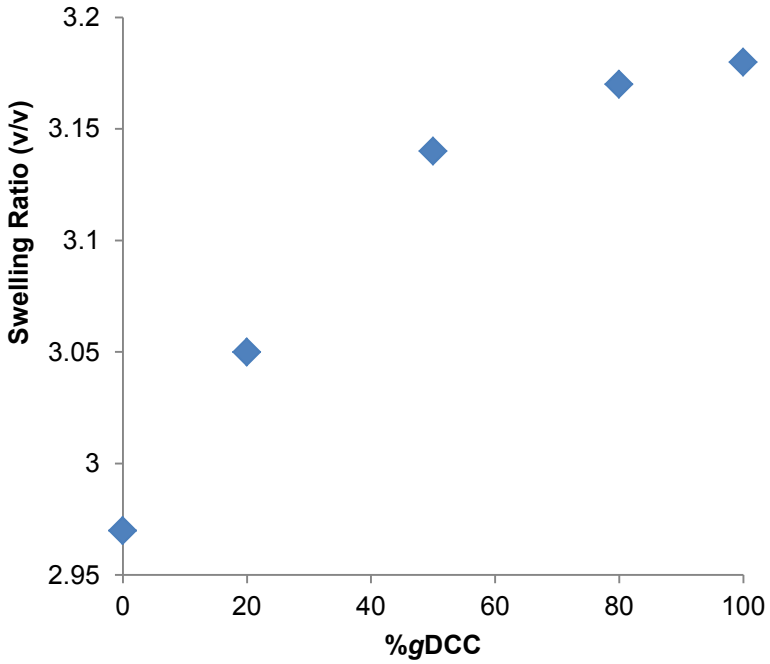


b)

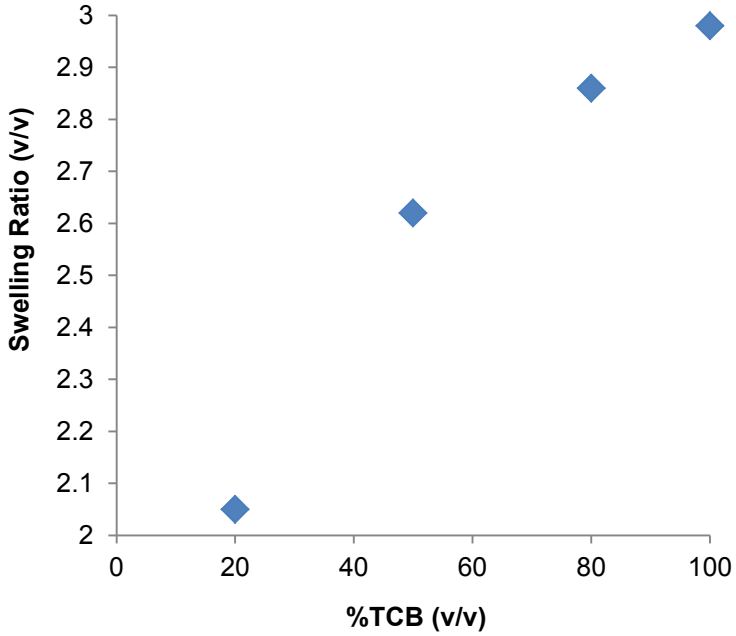


**Figure 2: Relationship between the SR and the % *g*DCC in the crosslinked polybutadiene. a) is the polymer series swelling in 100% TCB. b) is the 0% *g*DCC polybutadiene swelling in different %TCB in hexadecane.**

**Table 2: Mixed solvents used for swelling gels of different % *g*DCC in the polymer backbone to achieve SR = 3.**

| % *g*DCC | TCB: Hexadecane | SR |
|---|---|---|
| 0 | 100:0 | $2.96 \pm 0.04$ |
| 20 | 95:5 | $2.96 \pm 0.03$ |
| 50 | 85:15 | $2.95 \pm 0.01$ |
| 80 | 85:15 | $2.95 \pm 0.02$ |
| 100 | 85:15 | $2.96 \pm 0.03$ |

**Table 3: Solvents used for swelling the polymer series and the corresponding volume SR for hysteresis testing.**

| Polymer Series | Solvent | SR |
|---|---|---|
| 3A | TCB | $4.0 \pm 0.02$ |
| 3E | TCB:hexadecane (85:15) | $3.9 \pm 0.03$ |
| 4A | TCB | $4.1 \pm 0.02$ |
| 4B | TCB:hexadecane (95:5) | $4.2 \pm 0.02$ |
| 4C | TCB | $6.5 \pm 0.03$ |
| 4D | TCB | $6.4 \pm 0.01$ |

# *3. Dynamic Mechanical Testing*

## 3.1 Fracture Toughness Testing

### A. Background

In bulk materials, flaws act as stress-concentrators, creating localized stresses that are much greater than those in the bulk. These stress concentrators lead to the formation and growth of cracks, which ultimately cause the rupture of the material. Therefore, the crack growth behavior is an important factor in determining a material's toughness property.[22] Fracture toughness is used to describe the energy required to propagate an existing flaw, which is defined as the critical energy released per unit area increase during the crack growth.

The classic fracture toughness test, and that used here, is based on the Thomas-Rivlin model.[23] Two sample films are tested. The films are identical in shape, except that one has a cut from one end to the middle and the other does not (Figure **3**).

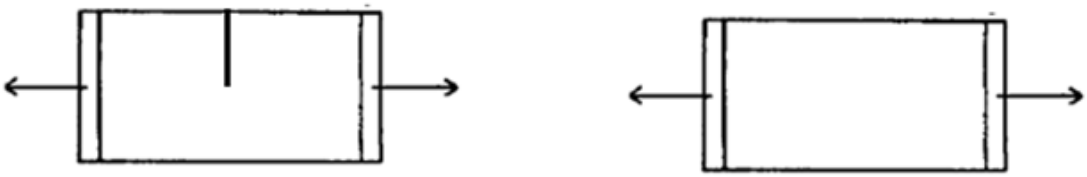


**Figure 3:[23] Schematic diagrams of test-pieces. Two films are identical in shape. The one on left has a cut in the middle formed with a razor blade, while the one on the right is an intact piece from the same material.**

Sample **1** is cut in the middle to dictate the maximum flaw in the material and determine the critical propagation strain, at which the cut starts to grow catastrophically under stress. Sample **2** is used to determine the strain energy density of the material. Stress-strain curves are plotted from both tests, and the modulus is obtained from the initial slope of sample **2.** The fracture toughness is calculated following eqn (2).

$$\left(\frac{\partial W}{\partial c}\right)_1 = -W_0 l_0 t \tag{2}$$

In eqn (2), $W_0$ is the energy density of sample **2** at the same strain as that in sample **1** when the crack starts to propagate. In general, $W_0$ can be obtained by graphical integration under the stress-strain curve for the uncut sample. $l_0$ is the initial distance between the clamps and $t$ is the thickness of the sample. The fracture toughness is defined as $W_0 l_0$.

**B. Tensile Testing**

The polymer films were cut into rectangular shapes and swollen in specific solvents. Once fully swollen, the polymer was cut into 2.5 mm×12 mm×0.5 mm sheets for tensile testing. The testings were performed using a Micro-Strain Analyzer (TA Instruments RSA III, New Castle, DE) at room temperature and 1 atm. The pulling rate was set at 5 μm/s. Nominal stress was plotted against percentage strain for each test. Young's modulus was obtained from the slope of the curve in the elastic range. Fracture toughness was calculated following the Thomas-Rivlin model.[23]

**3.1.1 Fracture Toughness of Polymers with *g*DCC Incorporated in the Backbones**

First the polymers with *g*DCC incorporated in the backbones were tested (swollen in DCB, decalin and TCB/hexadecane mixed solvent). Results were collected in Table **4**, Table **5** and Table **6**, respectively. The relationship among critical propagation point, modulus, fracture toughness and the *g*DCC percentage are shown in Figure **4** to Figure **8**. In the DCB and decalin series, with more *g*DCC incorporated, the modulus decreased whereas the critical propagation strain and fracture toughness increased.

**Table 4: Tensile testing results from polymers 3a to e fully swollen in DCB. All data were averaged over 7 experiments.**

| Mechanophore percentage | % strain | Young's Moduli ($\times 10^4$ Pa) | Fracture Toughness ($\times 10^3$ J/m$^2$) |
|---|---|---|---|
| 0% | 6.7 | 2.8 | 1.4 |
| 20% | 9.0 | 2.9 | 2.4 |
| 50% | 9.4 | 2.6 | 2.0 |
| 80% | 10.8 | 2.4 | 2.7 |
| 100% | 11.8 | 2.4 | 2.8 |

**Table 5: Tensile testing results from polymers 3a to e fully swollen in decalin. All data were averaged over 7 experiments.**

| Mechanophore percentage | % strain | Young's Moduli ($\times 10^4$ Pa) | Fracture Toughness ($\times 10^3$ J/m$^2$) |
|---|---|---|---|
| 0% | 6.7 | 3.0 | 2.5 |
| 20% | 9.0 | 2.9 | 2.9 |
| 50% | 9.4 | 2.6 | 3.1 |
| 80% | 10.8 | 2.2 | 3.5 |
| 100% | 11.8 | 2.6 | 3.5 |

**Table 6: Tensile testing results from polymers 3a to e fully swollen in the mixed solvents of TCB and hexadecane. All data were averaged over 4 to 6 experiments.**

| Mechanophore percentage | %strain | Young's Moduli ($\times 10^4$ Pa) | Fracture Toughness ($\times 10^3$ J/m$^2$) |
|---|---|---|---|
| 0% | 10.6 | 3.0 | 2.7 |
| 20% | 10.5 | 2.9 | 2.9 |
| 50% | 11.2 | 2.8 | 2.9 |
| 80% | 11.4 | 2.8 | 3.0 |

The differences in modulus and fracture toughness among different mechanophore percentages are caused by the solvent effect, which was later confirmed by the result when using mixed solvent to achieve the same SR. As shown in Figure **8**, the modulus and toughness are the same for all polymers in the series kept at constant SR, within a 95% confidence interval according to both a T-test and Q-test.

Based on the theory, both $l_o$ and $t$ of the film should be as small as possible relative to the width of the film.[23] Also, $l_o$ should be larger than the radius of the plastic zone at the tip of the cut. In this case, $l_o$ was set at 2.500 mm for each test, which is greater than the radius of the plastic zone (0.2 mm) calculated by Irwin's plastic zone correction.[24] Moreover, it is easy to mount the sample on the instrument with this distance for relatively consistent results.

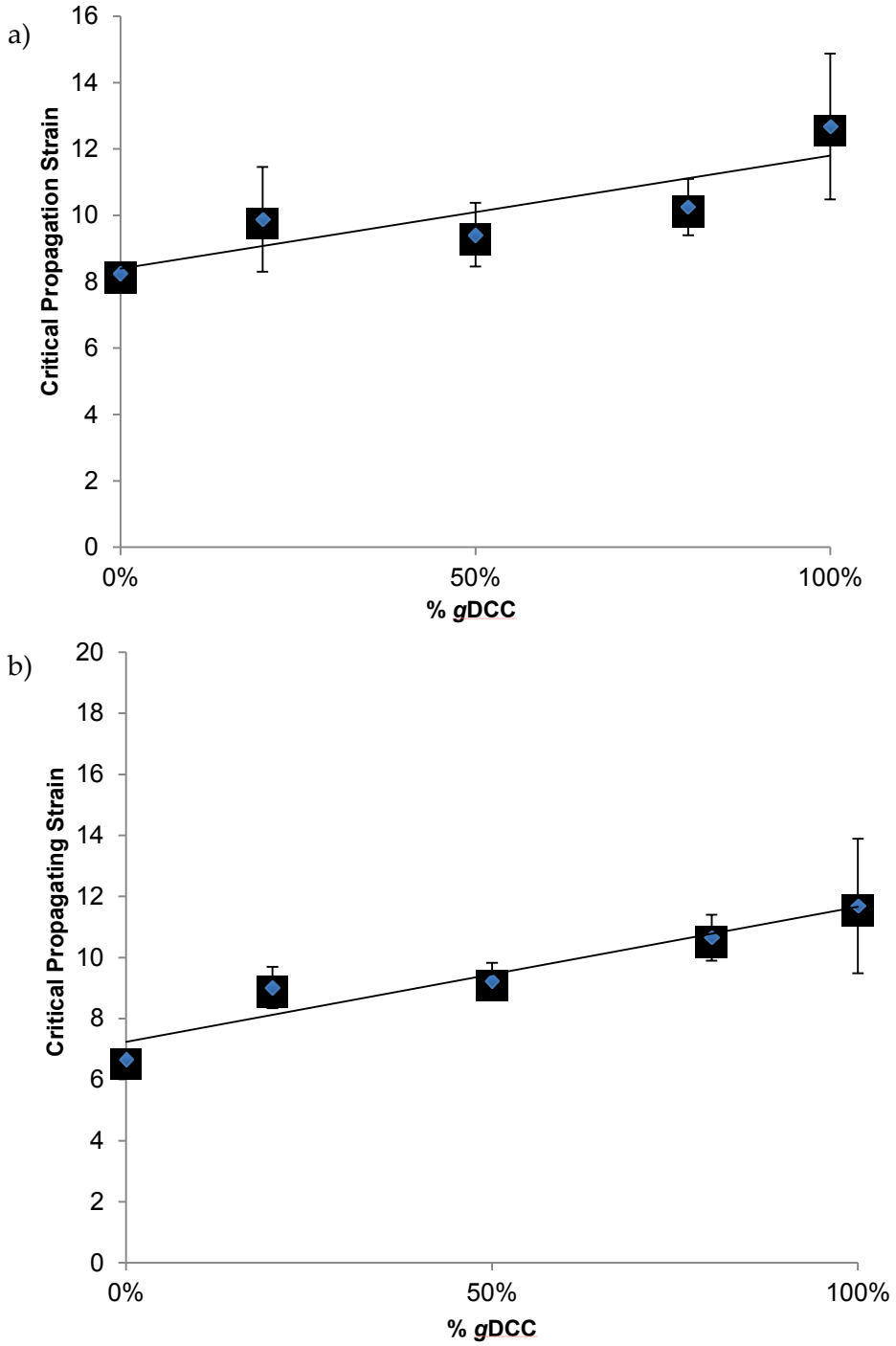


**Figure 4: Relationship between the critical propagation strain and the % *g*DCC in the crosslinked polybutadiene. Polymers were fully swollen in the DCB (a) and decalin (b). Line is provided to guide the eye.**

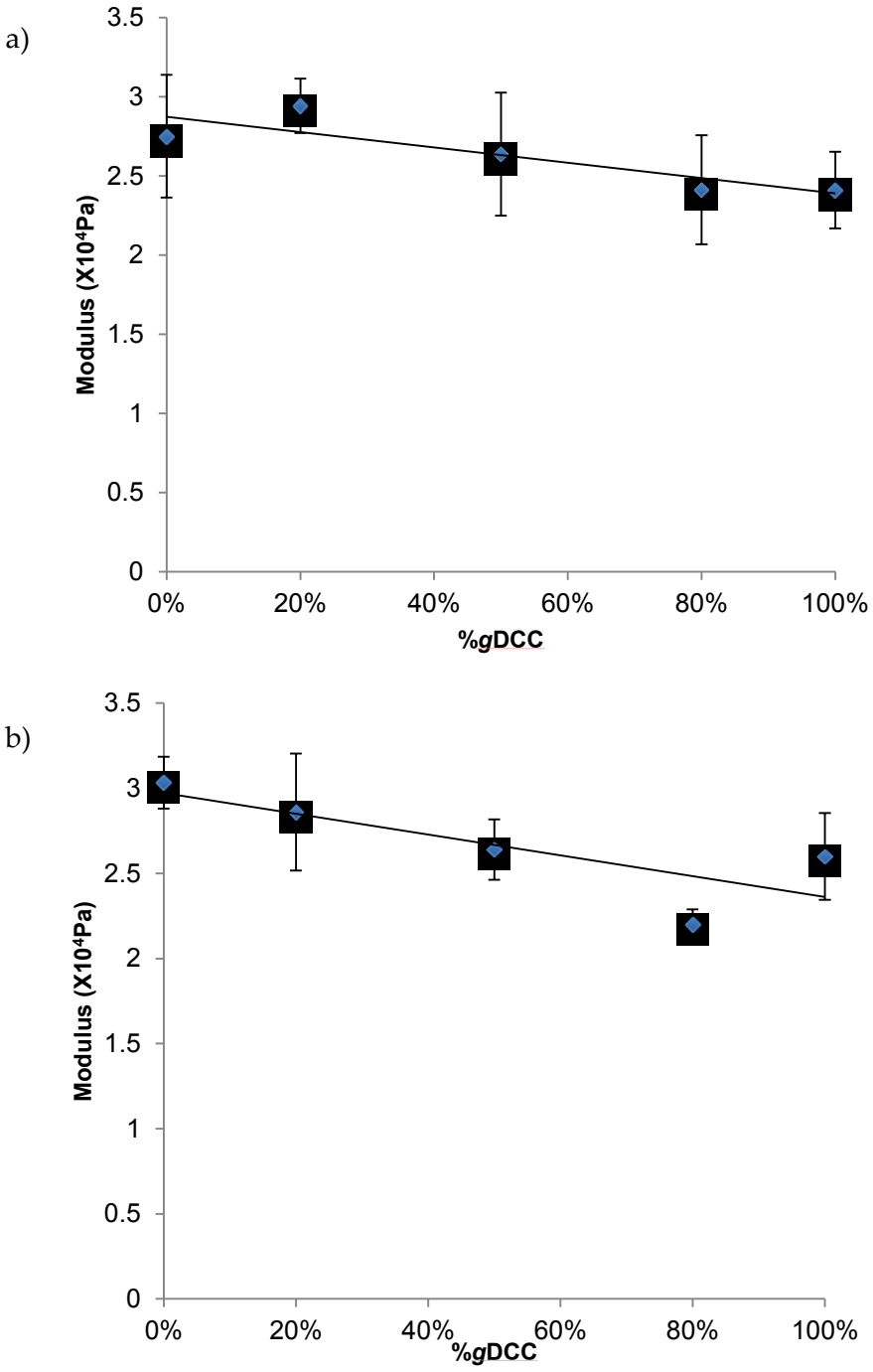


**Figure 5: Relationship between the modulus and the %*g*DCC in the crosslinked polybutadiene. a) Polymers were fully swollen in the DCB. b) Polymers were fully swollen in decalin. Line is provided to guide the eye.**

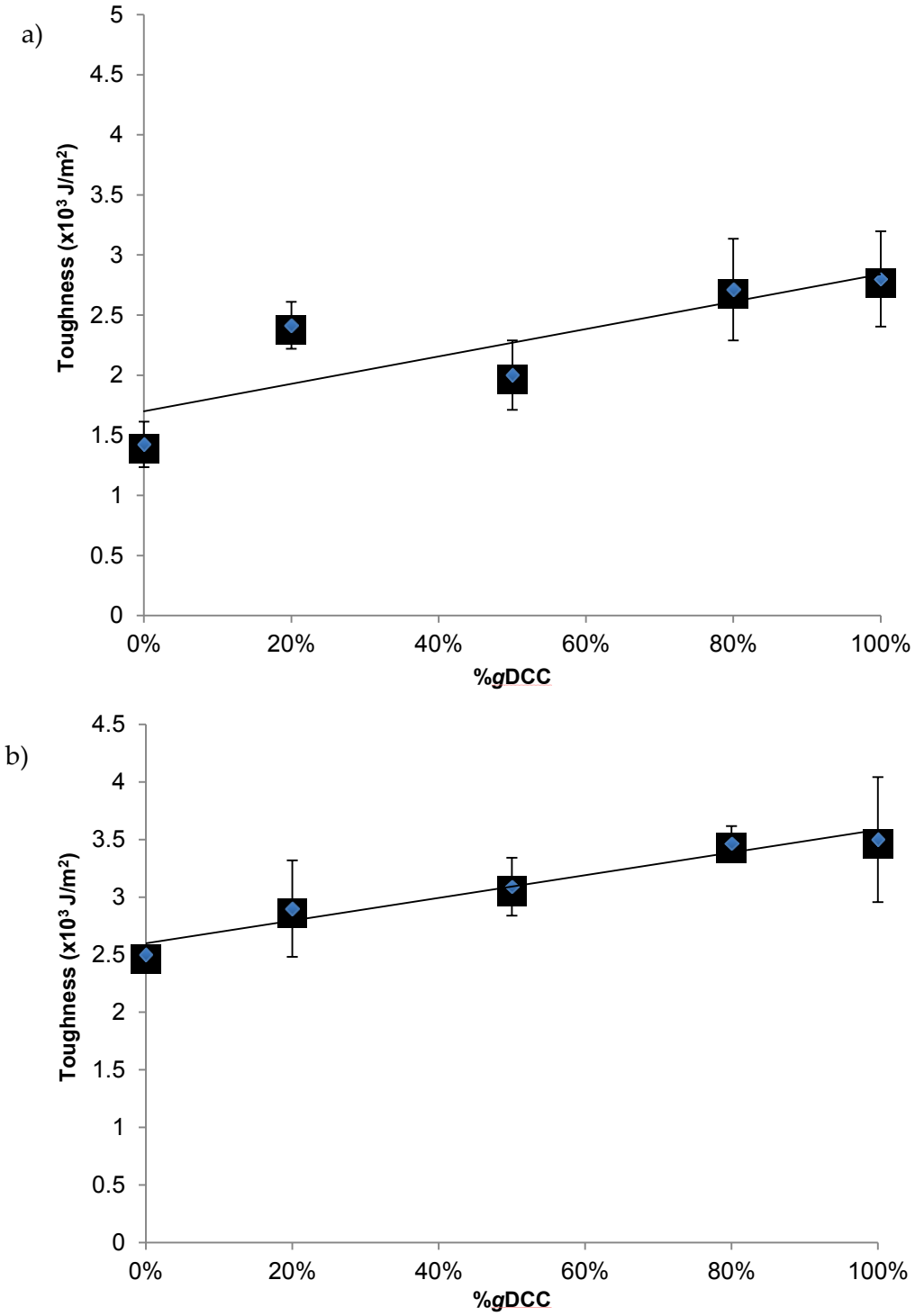


**Figure 6: Relationship between the fracture toughness and the %*g*DCC in the crosslinked polybutadiene. a) Polymers were fully swollen in the DCB. b) Polymers were fully swollen in decalin. Line is provided to guide the eye.**

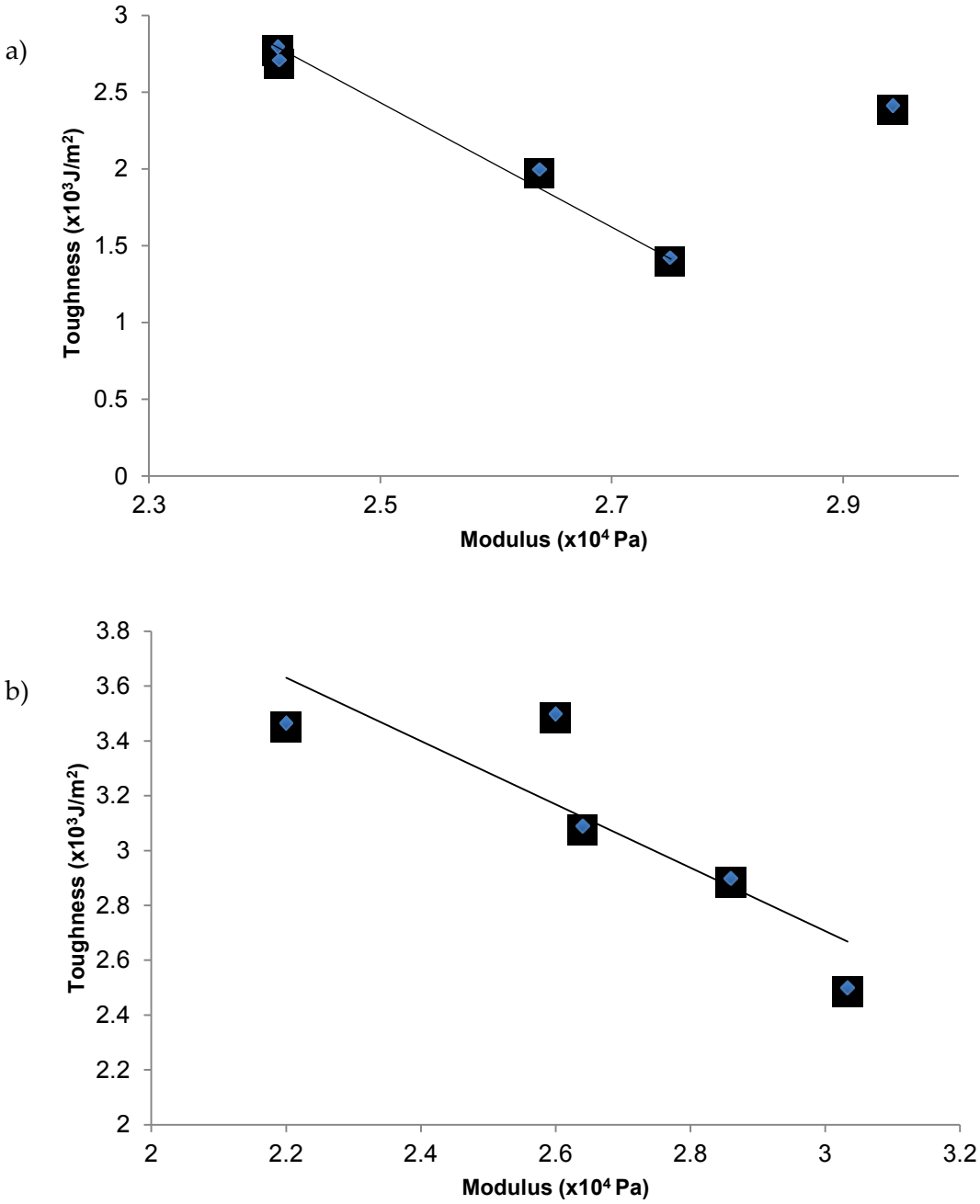


**Figure 7: Relationship between fracture toughness and modulus for polybutadiene with different percentages of *g*DCC. a) Polymer was fully swollen in DCB. b) Polymers were fully swollen in decalin. Data from 20% *g*DCC (Figure a, right most point) is an outlier, which was not included when the trend line was postulated. Line is provided to guide the eye.**

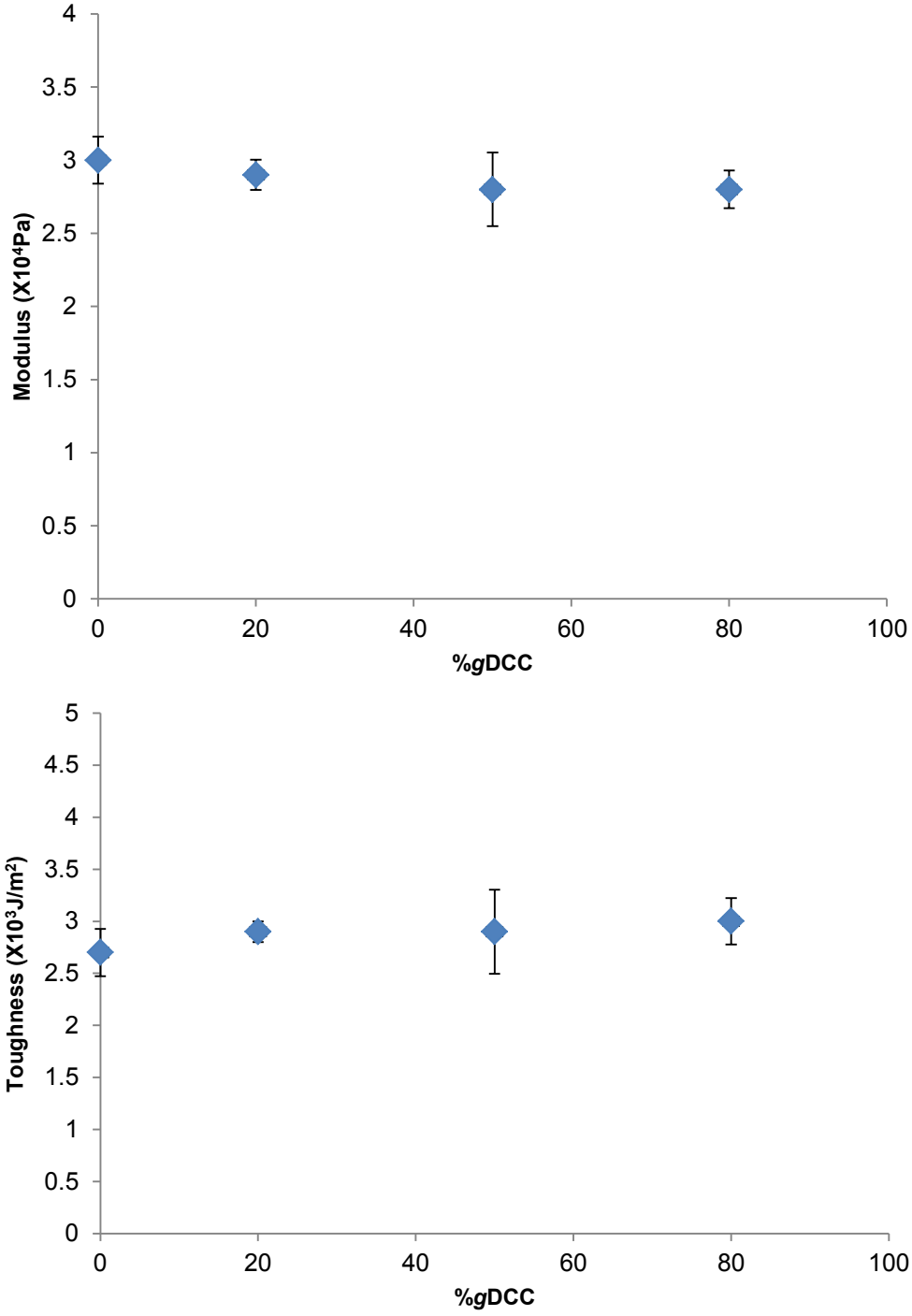


**Figure 8: Modulus and fracture toughness as a function of %gDCC. The polymers were swollen in mixtures of TCB and hexadecane to achieve SR = 3.**

### 3.1.2. Fracture Toughness of Polymers with *g*DCC Incorporated in the Crosslinking Position

Since the mechanical properties remain constant for all the polymer series, we hypothesize that the internal stress generated by the macroscopic deformation concentrated on the relatively short segments in the network. As a result, we incorporated the *g*DCC in the crosslinking position in the network and conducted similar fracture toughness testing to investigate the modulus and toughness trend. The results are shown in Table **7**. The Young's modulus and fracture toughness of **4c** and **4d** were indistinguishable under the testing conditions under 95% confidence interval according to the T-test.

**Table 7: Tensile testing results from polymers 4a and 4b fully swollen in TCB and hexadecane. All data were averaged over 5 experiments.**

| Polymer samples | % Critical Strain | Young's Modulus ($\times 10^4$Pa) | Fracture Toughness ($\times 10^3$J/m$^2$) |
|---|---|---|---|
| 4a | 7.8 ($\pm$0.4) | 2.2 ($\pm$0.2) | 1.6 ($\pm$0.2) |
| 4b | 8.3 ($\pm$0.2) | 2.1 ($\pm$0.1) | 1.7 ($\pm$0.1) |

## 3.2 Cyclic Tensile Testing

### A. Background

One supposition why we did not encounter fracture toughness enhancement is that the critical strain in the fracture tensile testing is not high enough to trigger large amount of activations in the polymer network. As a result, we investigated cyclic tensile testing as a mimic of the fatigue process of the material.

In material science, fatigue is a process during which damage is accumulated in the imperfect parts (stress concentrators, *e.g.* surfaces, interfaces, persistent slip bands (PSBs)) of the material when subjected to cyclic loadings. In this case, samples are exposed to repeat tensile deformation without introducing any visible flaws into the film. We hoped that by adopting this method, we might raise the critical strain/stress during the test, as well as make more mechanophores experience the stress as an attempt to investigate the strain/stress effect on the *g*DCC activation.

### B. Tensile Testing

The polymer films were cut into ~50 mm ×12 mm ×0.5 mm sheets for tensile testing. The test was performed using a Micro-Strain Analyzer (TA Instruments RSA III, New Castle, DE) at room temperature and 1 atm. Nominal stress was plotted against strain for each test.

### 3.2.1 Rate Dependence Testing

The pulling and the relaxing rates were set at 1 μm/s, 2 μm/s, 5 μm/s, 10 μm/s, respectively. Nominal stress was plotted against strain for each test. Energy dissipated during each cycle was obtained from the difference in energy density (area under the stress/strain curve) between the straining and relaxing process. The purpose is to find the optimized loading rate under which the energy dissipation in the control samples are minimized, and maintain the same rate to test the *g*DCC incorporated samples to compare the difference in the energy dissipation caused by the mechanophore activation. The results are collected in Figure **9** and the energies dissipated for all the samples under different loading rates are shown in Tables **8** to **10**.

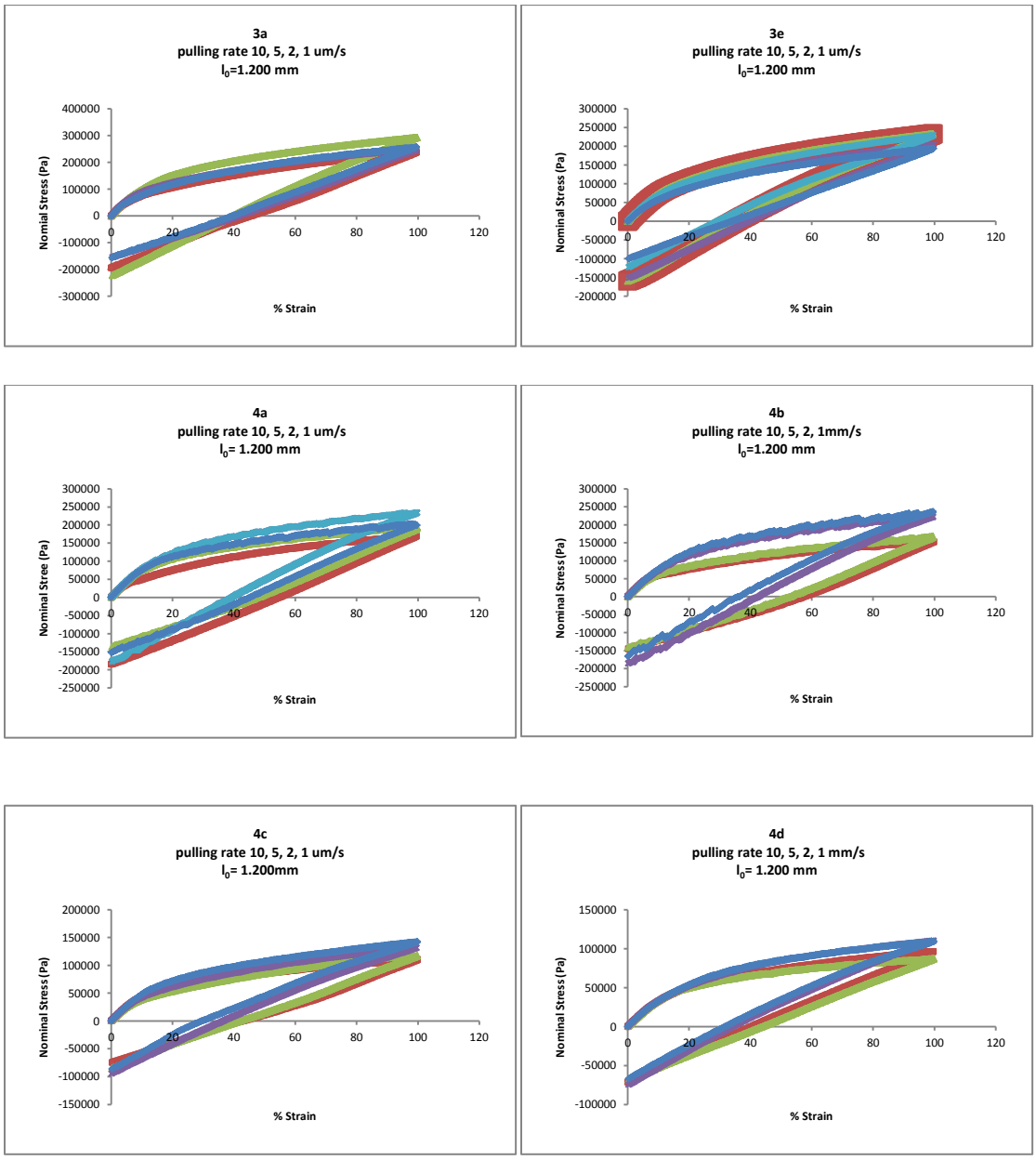


**Figure 9: Energy dissipation of the polymer series during one cycle of tension-relaxation under different strain rates.**

**Table 8: Energy dissipation of 3a and 3e.**

| Sample | Length (mm) | Loading Rate (μm/s) | Energy Released ($\times 10^6$ J/m$^3$) |
|---|---|---|---|
| 3A -1 | 1.2 | 10 | 9.6 |
| 3A -2 | 1.2 | 5 | 11.2 |
| 3A -3 | 1.2 | 2 | 10.2 |
| 3A -4 | 1.2 | 1 | 9.5 |
| 3E -1 | 1.2 | 10 | 8.0 |
| 3E -2 | 1.2 | 5 | 7.3 |
| 3E -3 | 1.2 | 2 | 6.9 |
| 3E -4 | 1.2 | 1 | 6.8 |

**Table 9: Energy dissipation of 4a and 4b.**

| Sample | Length (mm) | Loading Rate (μm/s) | Energy Released ($\times 10^6$ J/m$^3$) |
|---|---|---|---|
| 4A-1 | 1.2 | 10 | 7.6 |
| 4A-2 | 1.2 | 5 | 9.0 |
| 4A-3 | 1.2 | 2 | 9.0 |
| 4A-4 | 1.2 | 1 | 9.0 |
| 4B-1 | 1.2 | 10 | 7.6 |
| 4B-2 | 1.2 | 5 | 7.8 |
| 4B-3 | 1.2 | 2 | 8.8 |
| 4B-4 | 1.2 | 1 | 8.4 |

**Table 10: Energy dissipation of 4c and 4d.**

| Sample | Length (mm) | Loading Rate (μm/s) | Energy Dissipation ($\times 10^6$ J/m$^3$) |
|---|---|---|---|
| 4C-1 | 1.2 | 10 | 5.0 |
| 4C-2 | 1.2 | 5 | 4.6 |
| 4C-3 | 1.2 | 2 | 4.5 |
| 4C-4 | 1.2 | 1 | 4.6 |
| 4D-1 | 1.2 | 10 | 3.9 |
| 4D-2 | 1.2 | 5 | 3.9 |
| 4D-3 | 1.2 | 2 | 3.8 |
| 4D-4 | 1.2 | 1 | 3.6 |

As shown in Tables **8** to **10,** there is no significant correlation between the energy dissipation per unit volume and the loading rate among the tested samples. What needs to be pointed out is that all of the tests conducted under different rates for a certain kind of polymer were collected from the same sample. The gap distance was reset at 1.200 mm before the start of each loading cycle.

### 3.2.2 Cyclic Tensile Testing

The same polymer series was subjected to multiple tension-relaxation loading cycles, in an effort to stretch the polymer chains to the maximum extension before failure and explore the unit energy dissipation difference between targeted polymers and control polymers to investigate whether this extreme condition can activate the mechanophore in the polymer system. Each sample was set at 1.200 mm initially and deformed to 100% strain. Then it was relaxed to the strain for which the stress is equal to 0 and subjected to another cycle. This process was repeated until the polymer failed. The unit energy dissipation for each cycle, number of cycles survived, total energy dissipation, critical strain and critical stress are shown in Table **11** and Figure **10**.

**Table 11: Testing conditions and results across the polymer series.**

| Sample # | Loading Rate ($s^{-1}$) | Total Energy Dissipation ($\times 10^6$ J/m$^3$) | Length $l_0$ (mm) | loading cycles | Ultimate Strain (%) | Ultimate Stress ($\times$ $10^5$ Pa) |
|---|---|---|---|---|---|---|
| 3A | 1 | 58.82 | 1.200 | 7 | 182 | 2.32 |
| 3E | 1 | 106.77 | 1.200 | 13 | 459 | 3.49 |
| 4A | 1 | 102.31 | 1.200 | 20 | 409 | 2.98 |
| 4B | 1 | 45.42 | 1.200 | 8 | 291 | 2.71 |
| 4C | 1 | 42.84 | 1.200 | 12 | 546 | 2.80 |
| 4D | 1 | 22.31 | 1.200 | 8 | 337 | 1.88 |

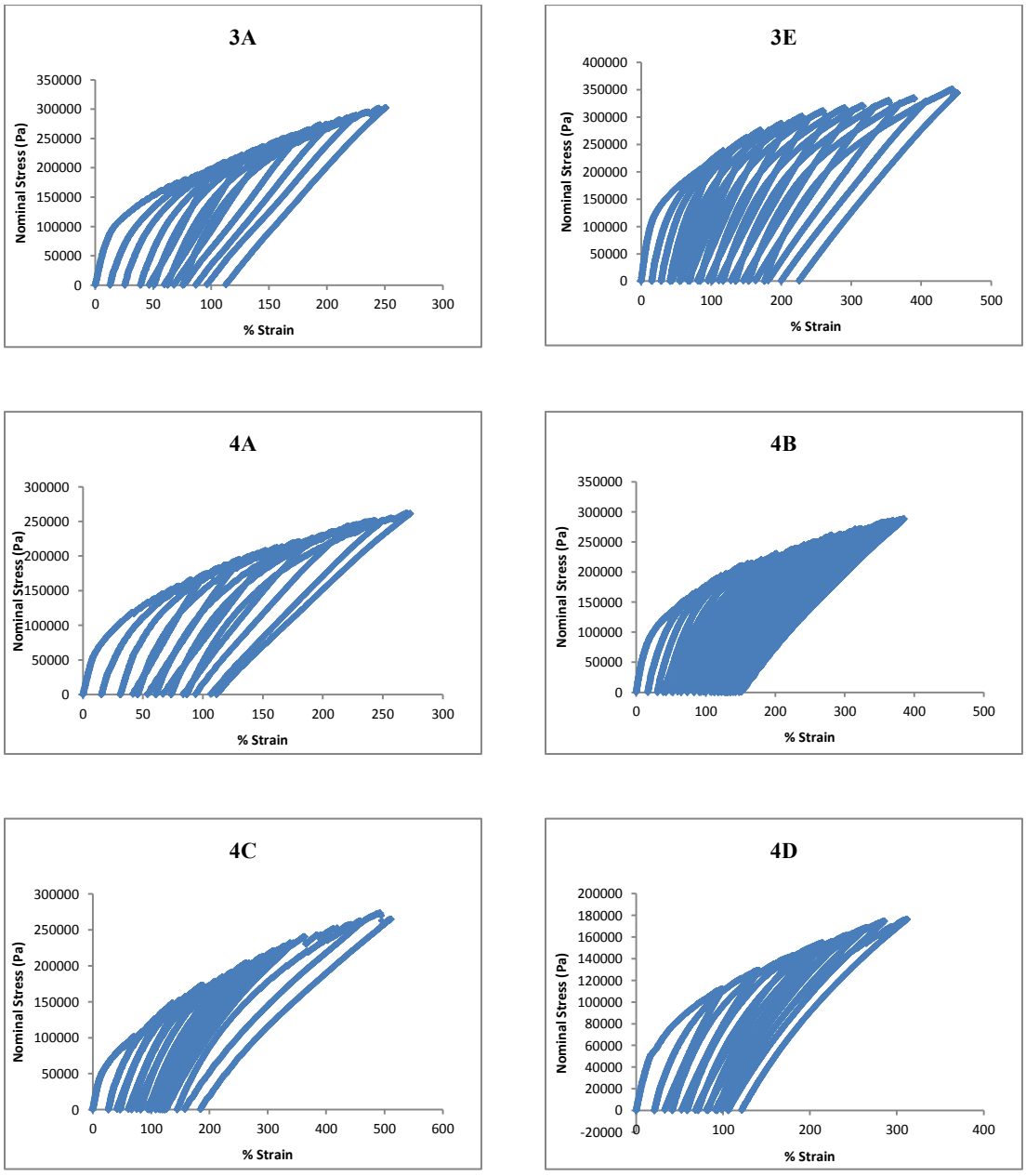


**Figure 10: Hysteresis cycles for the control and mechanophore incorporated polymers, each time the sample was strained to 100% under tensile loading. The energy dissipation was calculated by subtracting the elastic energy stored during straining from the external work done to the system. The materials were considered to be incompressible.**

As shown in Table **11** and Figure **10**, with *g*DCC in the polymer backbones, the energy dissipation increased by twice and the ultimate stress and strain increased as well. In the case where *g*DCCs were incorporated in the crosslinking position, however, the trend is the opposite: mechanical properties decrease, which was unexpected. Possible reasons for this result are described in the discussion section.

## *4. Structural Characterization*

### 4.1 NMR Characterization

In order to further investigate whether there are activations in the polymer network, **3a** and **3e** with *g*DCC incorporated in the polymer backbones were hydrolyzed with tetrabutylammonium hydroxide (TBAOH) in THF overnight,[25] precipitated with methanol, and dissolved in *d*-chloroform to obtain the NMR spectra. As shown in Figure **11** and **12**, no matter whether the sample was taken from the cut or uncut area of the cut samples, or from the uncut samples (Figure **13**), there are no new detectable peaks ($\delta$ = 4.48 or $\delta$ = 5.84) in the spectra that would be diagnostic for activation of *g*DCC.

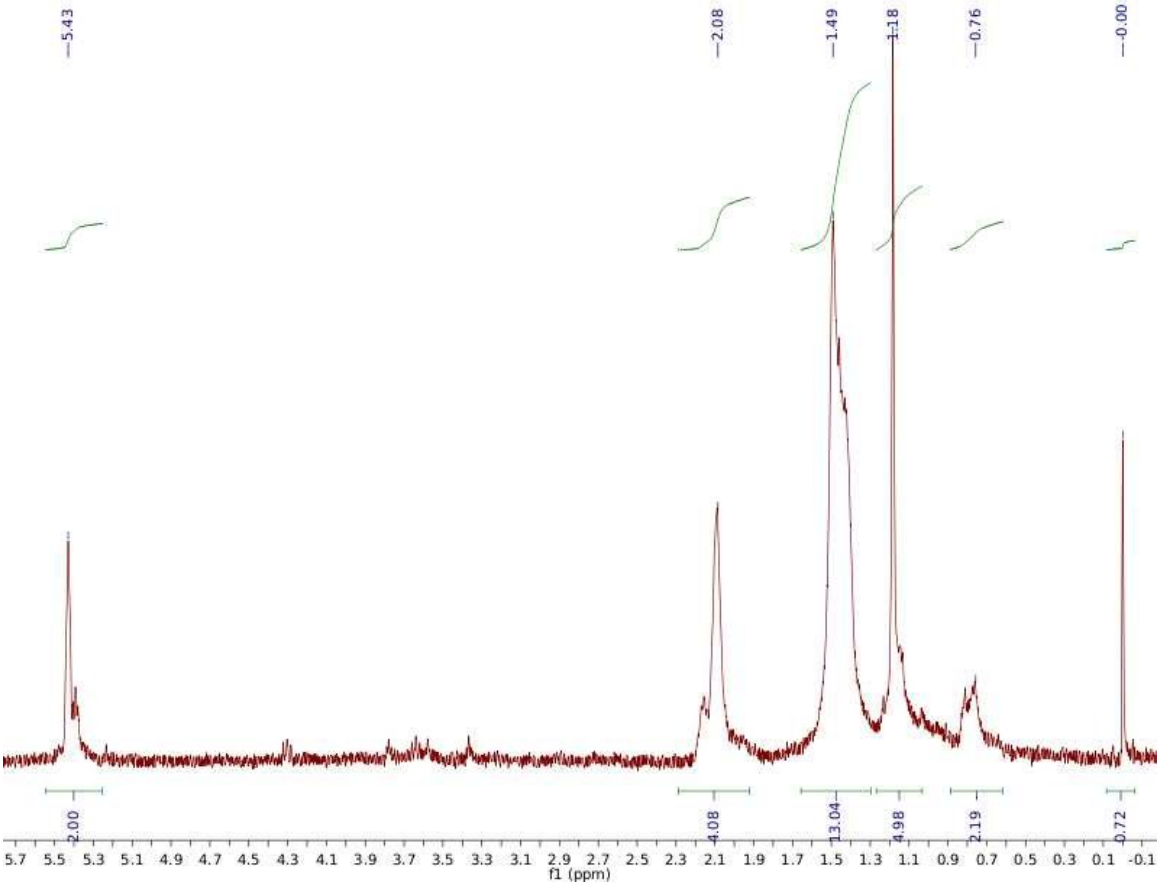


**Figure 11: NMR spectrum of failed samples near the crack surface.**

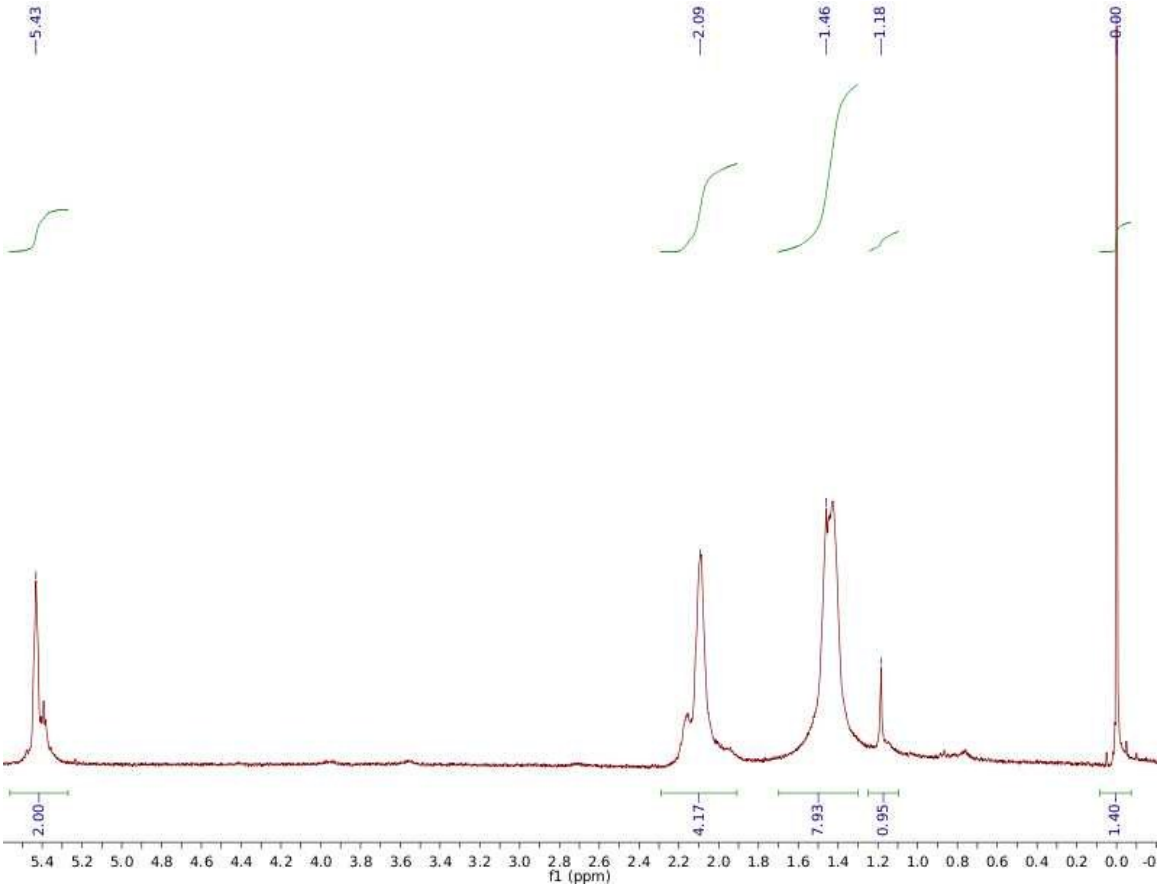


**Figure 12: NMR spectrum of failed samples away from the crack surface.**

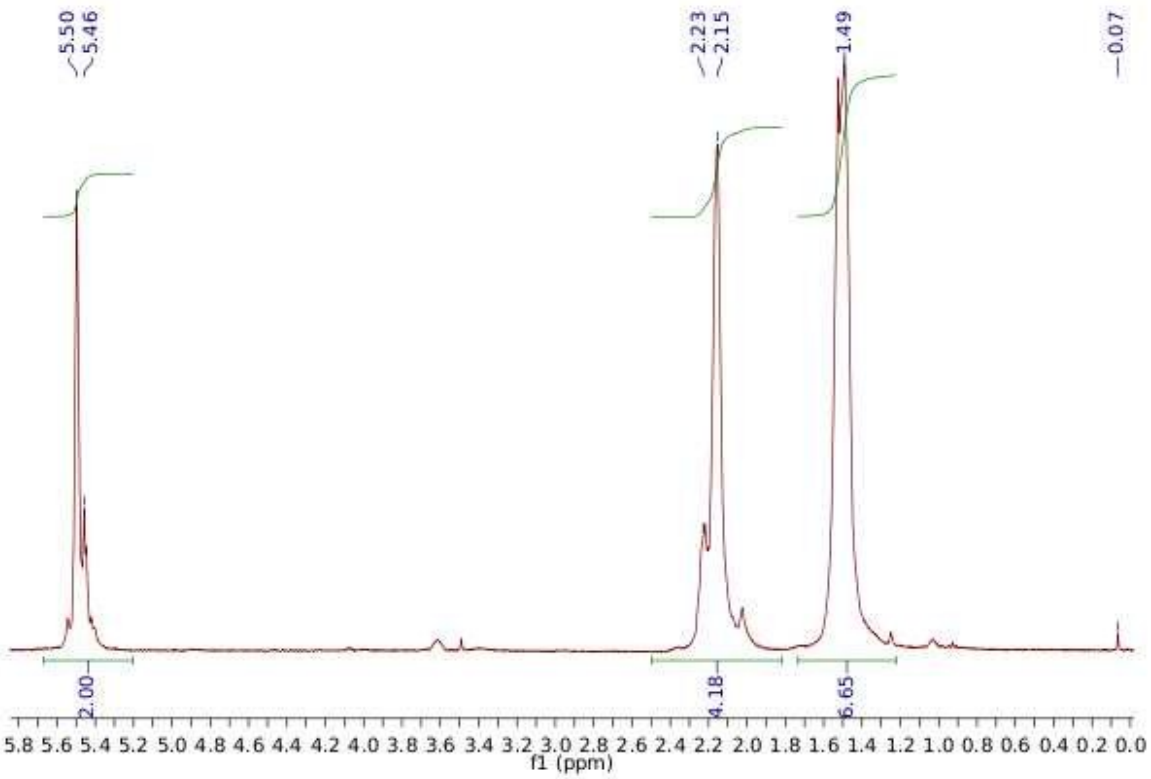


**Figure 13: NMR spectrum of uncut samples after testing.**

## 4.2 FT-IR Characterization

Since the crosslinking densities of **4a** and **4b** are only 4% (molar ratio)**,** the *g*DCCs in the crosslinkers are insufficient to obtain the NMR spectra. As a result, we turn to FT-IR spectroscopy to look for differences between samples before and after tests, and looking for the characteristic peaks corresponding to alkyl chlorides. As shown in Figure **14** and **15**, the peaks are normalized to 1460 $cm^{-1}$. The intensity of the C-Cl stretch (677 $cm^{-1}$) decreases slightly (0.511 to 0.508) after tensile testing, which is not significant to conclude the *g*DCC mechanophores have been activated in the gel.

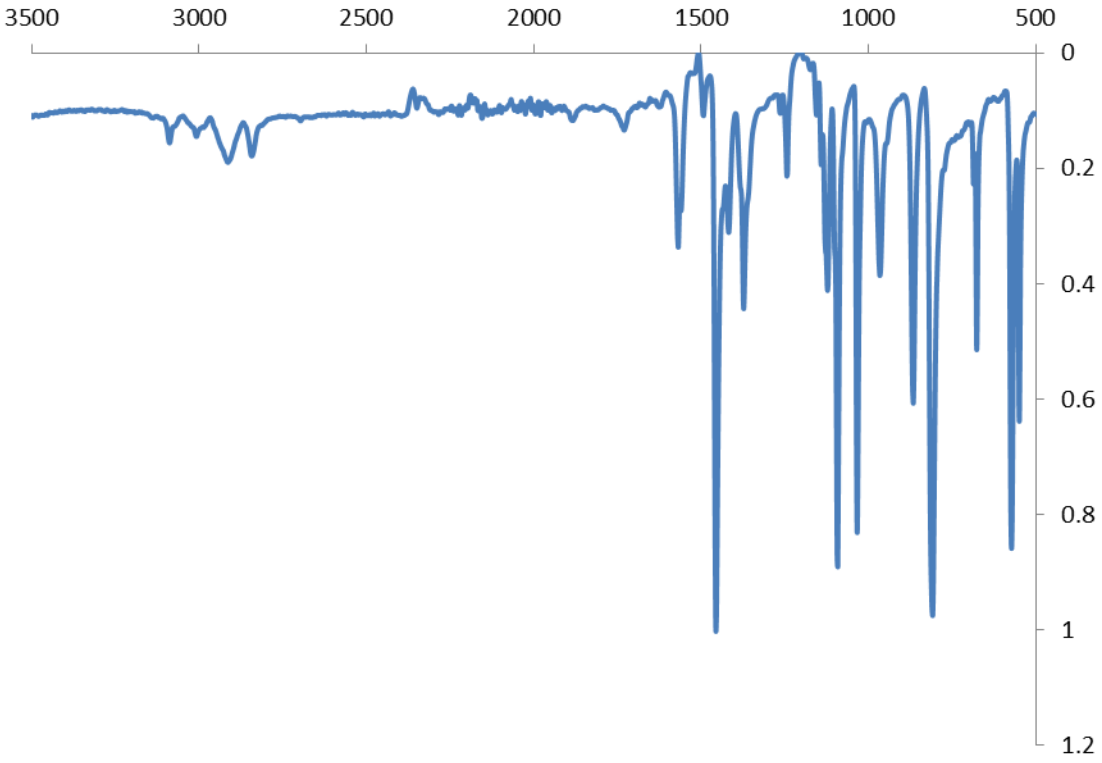


**Figure 14: FT-IR spectrum for 4a before fracture tensile testing.**

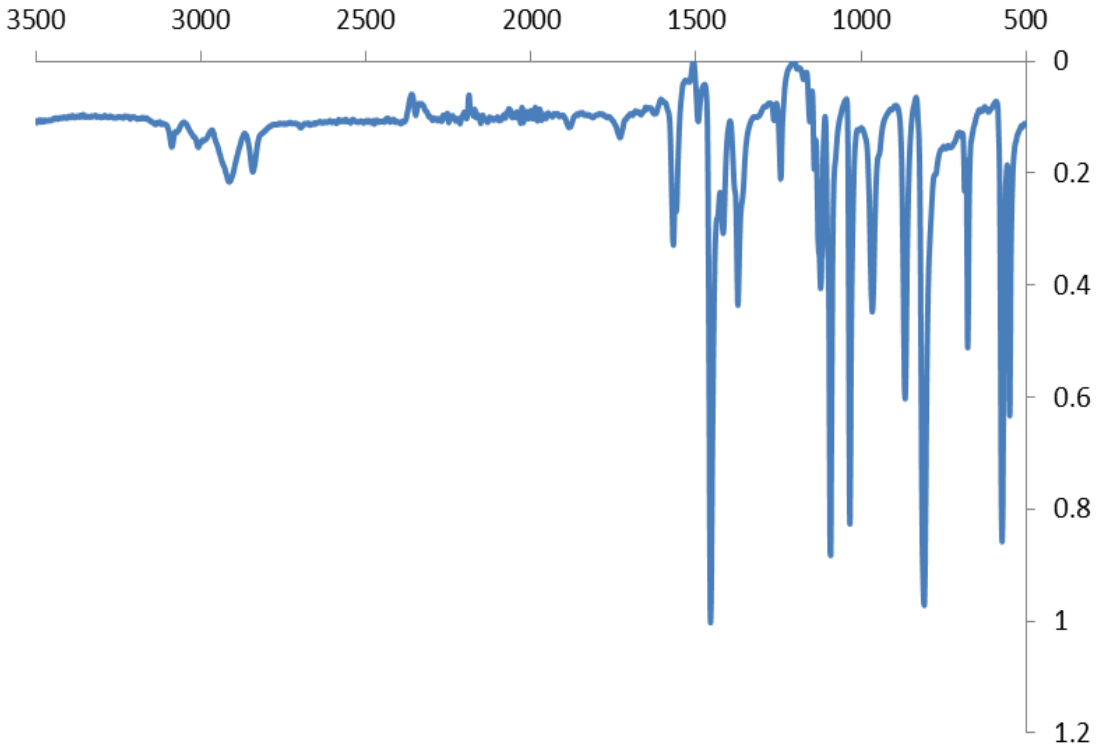


**Figure 15: FT-IR spectrum for 4a after fracture tensile testing near crack surface.**

# III. Discussion

## *1. Solvent Choice and Swelling Ratio Investigation*

Table **1** shows that with more *g*DCC incorporated, the polymers' SRs increase in most solvents. This result poses a difficult challenge for comparing the modulus and fracture toughness among all of the fully swollen polymers due to the effect of SR on these properties. Since we only want to see the mechanophore activation effect, the main function of the solvent is to minimize other effects, such as chain-chain interactions, on the mechanical properties and make the crosslinking density the only dominant factor. As a result, SR would ideally be constant for all polymers in a series. Four attempts were made to achieve this goal.

Our first attempt was to stoichiometrically add solvent to the polymers with different percentages of mechanophore to achieve the same SR to investigate whether it would distribute evenly over time. DCB and decalin with 100% mechanophore containing polymers were used for this attempt. Since the volume of solvent is between 1 and 3 mL, it is difficult to balance the competition between evaporation and absorption. The film initially swelled unevenly, and after 2 h the majority of the solvent had evaporated, but the polymer was still distorted.

Our second attempt was to conduct polymerization in the intended amount of solvent, and polymers containing 100% mechanophore were polymerized in decalin. When only the monomers existed during polymerization in the oven, the total mass loss

is around 1%. Polymerization in solvent, however, resulted in a loss of total mass of 30%. These results indicate that solvent evaporation proceeds at the polymerization temperature. Monomers do not evaporate much during polymerization, not because they have low vapor pressure (in fact their vapor pressures are higher than the solvents used), but likely due to the fact that the polymerization proceeds quickly and inhibits the evaporation.

Our third attempt was to run tests at different SRs. If the toughness and modulus of the same polymer had quantitative trends as a function of SR, we could extrapolate the properties of different polymers to the same SR. We recognized two main challenges to this approach. First is the homogeneity of the solvents in the polymer. For good solvents, before the polymer is fully swollen, the solvent is unevenly distributed in the polymer, making the polymer distorted in shape and not suitable for tensile testing. This phenomenon disappeared after the polymer was fully swollen. Second is the preservation of the partially swollen polymer. It is hard to find a solvent that produces a great SR and has a low vapor pressure at the same time. In the previous experiments using DCB and decalin, when the fully swollen polymer was exposed to open air, it started to lose solvent extremely fast and the polymer was likely to distort. Consequently, it can also affect the reliability of the results from the tensile testing. Several attempts show the results are sporadic and non-reproducible.

After more consideration, mixed solvents of TCB and hexadecane were used as the swelling solvents, which constituted our fourth attempt. This strategy seems promising since using mixed solvents is a simple and straightforward way to control the solvents uptake. TCB and hexadecane both have low vapor pressures but vary largely in swelling capabilities. The only concern is that different solvent mixture will have different effects on the mechanical properties and affect the final results. This concern will be verified by using different mixed solvents to achieve the same SR and see whether there is a difference.

## *2. Tensile Testing*

In my research the crosslinkers were introduced as a modification to the polymer structure. As experimentally demonstrated by other groups,[13,26] networks lead to greater mechanophore activation then linear polymers. Representative examples include elastomeric spiropyran-linked poly(methyl acrylate) (PMA) polymers being activated under uniaxial tension or cyclic loading vs. spiropyran crosslinked poly(methyl methacrylate) (PMMA) being activated under compression[12] and 1,2-dioxetane-linked PMA vs. 1,2-dioxetane crosslinked PMA being activated under uniaxial tension.[13] In these examples, the mechanophore was either incorporated in the backbone of the linear polymer material, or in the crosslinking position in the crosslinked polymer. Larger percentages of mechanophores were activated in the latter situation. It can be understood from both the topology and relaxation times of the system. In the

crosslinked material, weak bonds in the mechanophores necessarily break when local stress is increased beyond a certain threshold value. For linear polymers above their $T_g$, however, disentanglement by chain reptation is an effective mechanism to reduce stress on the polymer chains, and as a result the percentage of mechanophore activation is smaller.

## 2.1 Fracture Toughness Testing

Figures **5** through **9** suggest that the mechanophore incorporation has an effect on the modulus and fracture toughness of the crosslinked polymer. Variations can be observed among polymers with different mechanophore content. The increase of the critical propagation strain and the decrease of the modulus suggest that the polymers with *g*DCC are more elastic than those without it. The fracture toughness of the polymers increase which is consistent with our hypothesis. The decrease of the modulus was expected as well since moduli should theoretically decrease with increased swelling.[27] Comparing the results of two series, the DCB swollen polymers exhibit a better trend than those swollen by decalin. There are three possible reasons for these observed differences. The first one is the evaporation of the solvent. Due to the fact that the vapor pressure of decalin is higher than that of DCB, during the tensile testing the polymer may undergo constant evaporation and make the results non-reproducible. The second reason is the effect of the BHT additive in the decalin series. BHT was used to prevent the polymer from being photocrosslinked when exposed to light. It might,

however, affect the modulus and toughness of the polymer as well. The last reason is the difference of the polymer SRs. Since decalin provides a relatively small SR, it might not extend the polymer network enough to overcome the chain-chain interactions, and those in turn might contribute to the observed properties.

To test if the modulus and toughness changes are due to the solvent, polymers swollen in mixed TCB and hexadecane with the same SR were tested. As shown in Figure **8**, the modulus and toughness have the same qualitative trend as before, but the difference is not statistically significant. The possible reason for this may be insufficient strain transferred to the mechanophore in the backbones when the material was torn apart, and the strain was mainly focused on the crosslinkers in the polymer. Before the strain reaches the critical value to activate the mechanophore, the crosslinkers may already break.[19]

As a result, we designed *g*DCC-crosslinked polybutadiene polymers and conducted similar tensile testing, in an effort to explore whether the stress actually focuses on the crosslinker in the material and can activate the *g*DCC mechanophore, which in turn changes the mechanical properties of the material. As shown in Table **7**, for polymer **4a** and polymer **4b** at the same SR, the fracture toughness properties do not differ on a detectable level from those of control polymers in which the crosslinkers do not have *g*DCC incorporated. The possible reasons for this are discussed as follows.

First is the limitation of the polymer structure. In the case of our system, the material is very rigid and brittle. As demonstrated by Eyring,[28] in cases where a fairly rigid structure is being disrupted, a certain number of molecules will be displaced simultaneously with no more shearing force than would be expected for one. As a result, the internal stress is not evenly distributed in the polymer matrix and only a small amount of the mechanophores can be activated (most likely at the interfaces between layers of molecules that move simultaneously). Mechanical properties are probably not affected on a detectable level by these activations. As experimentally demonstrated by Chen *et al*,[13] a dioxetane mechanophore shows no activation in rigid glassy polymer samples under tensile deformation, including dioxetane-linked PMA and PMMA below their $T_g$, which is explained by a strong localization of strain so that only a small fraction of dioxetane scission events take place.

Another consideration is the limitation of the testing method. During the fracture toughness testing, an intentional crack is introduced into the material and the stress is highly concentrated on the tip of the crack as it grows. The activation will take place along the direction of the crack growth and only exist in the close area of the crack position. This phenomenon has already been discovered in other cases like spiropyran and dioxetane mechanophores incorporated polymers. So the question is whether the activations along the crack are sufficient enough to increase the fracture toughness of the polymer.

To explore this question, the theoretical value of energy release caused by the mechanophore activation was calculated. The value is an approximation based on our previous work on *g*DBC by SMFS,[14] with the following assumptions/approximations:

**1)** Toughness increment caused by one *g*DCC ring activation equals to that of one *g*DBC ring (1.05 Å extension along the force direction; ring opens under the force of 1.2 nN): In practice, the *g*DCC requires higher forces than *g*DBC for a given time scale, and the time scale here (s) is longer than in the SMFS (~10 ms)

**2)** Toughness increment of *g*DCC in single polymer chain equals that in a crosslinked polymer chain;

**3)** Ring opening reaction of *g*DBC and *g*DCC happening under the same stress are on the same time scale;

**4)** Toughness increment is proportional to the amount of *g*DCC being activated;

**5)** Composition of the crosslinked polymer is that of the monomers and crosslinkers added (i.e. everything reacted during synthesis).

According to these assumptions, the toughness increment caused by one *g*DCC repeating unit equals to,

$1.2\ \text{nN} \times 1.05\ \text{Å} = 1.26 \times 10^{-19}\ \text{J}$

when the SMFS pulling rate is 3 μm/s.

For mechanophore incorporated in the polymer backbone, take 40% *g*DCC mechanophore incorporated crosslinked polybutadiene polymer for example, the mass percentage of the *g*DCC monomer equals to,

$Mw_{(gDCC\ monomer)} \times 80\% / (Mw_{(gDCC\ monomer)} \times 80\% + Mw_{(COD\ monomer)} \times 20\% + Mw_{(crosslinker)} \times 4\%)$

$Mw_{(gDCC\ monomer)}$: 191 g/mol

$Mw_{(COD\ monomer)}$: 108 g/mol

$Mw_{(crosslinker)}$: 349 g/mol

As a result, a polymer with a mass of 187.2 mg has 152 mg of *g*DCC monomer, corresponding to $7.95 \times 10^{-4}$ mol. The effective part being deformed is around 10% (portions of the sample between clamps). If all the *g*DCC mechanophores are activated, the added toughness should be,

$7.95 \times 10^{-4}$ mol $\times$ 1.26 $\times 10^{-19}$ J $\times$ $6.02 \times 10^{23}$ $mol^{-1} \times 10\% = 6$ J

Even with the uncertainty in the approximations, full *g*DCC activation could lead to theoretical additional toughness on the order of Joules per sample. The energy released during the cut growth of polymer is only on the order of $10^{-3}$ J, which is significantly smaller than the theoretical value available through mechanophore activation. In fact, activation as little as 0.1% of the mechanophores in the material might have a measurable effect on the toughness. The result further supports that the stress is not efficiently transferred to the mechanophore in the polymer backbones that activate enough *g*DCCs to increase the fracture toughness of the material.

For the *g*DCC in the crosslinker, a similar calculation was conducted and the added increment should be on the order of $10^{-1}$ J. The energy released during the cut growth of this polymer is on the order of $10^{-2}$ J, requiring an order of 10% of the crosslinking mechanophores to be activated, in order to contribute substantially to this value.

## 2.2 Cyclic Tensile Testing

For comparison, the SP and dioxetane mechanophore data in the PMA linear polymer chain and PMMA crosslinked polymer chain are considered here.[12] First, the activation energy the SP mechanophore is *ca.* $1.6 \times 10^{-19}$ J,[29] which is similar to that of *g*DCC activation. Second, in the SP-linked PMA polymer, the critical strain featuring the start of the mechanophore activation is *ca.* 200% and the activation reached a maximum value at *ca.* 1000% under the loading rate of 1.5 mm/s. For SP-crosslinked PMMA material the critical strain is *ca.* 20%, and at *ca.* 50% the activation increment reaches the maximum. The critical stress to activate the mechanophore in the crosslinked PMMA samples is *ca*. 50 MPa under the loading rate between 1 and 25 μm/s, while the critical stress for the linear PMA was not mentioned in the paper. For the dioxetane mechanophore,[13] in the crosslinked PMA film the critical stress is *ca.* 45 MPa, and 35 MPa for the linear dioxetane-linked PMA polymers under the loading rate of 8 $s^{-1}$. The activation energy and the critical strains were not mentioned in the paper. Compared with these results, the maximum strain and the maximum stress of our system in the

fracture toughness test are *ca.* 10% and 0.09 MPa under the loading rate of 1 μm/s, respectively. The energy input into the system is much smaller compared to the PMA and PMMA system. To what extent the mechanophore in the PMA and PMMA is activated has not been quantified. It is highly possible, however, the lower energy input in our system limits the *g*DCC mechanophore activation. As a result, a similar test to the SP tensile testing was conducted to achieve a higher energy input in our system, and the energy dissipation was compared between the control and the mechanophore incorporated polymers. As shown in Table **6**, among all the polymer series, only the polymer with *g*DCC in the backbone showed higher energy dissipation compared to the control polymer, all the *g*DCC-crosslinked polymers showed the opposite trend. The NMR characterization of the post-test samples showed no detectable activation of the *g*DCC mechanophore in the samples. The differences in the energy dissipation, ultimate strain and ultimate stress are possibly caused by the solvent used for swelling the polymers. Since the solvents to swell each kind of polymer are different, during deformation the interactions between solvent molecules, polymer matrix and the solvent molecules may vary to a large extent and affect the mechanical properties.

## *3. Molecular Characterization*

As shown in Figure **11** and **12**, no matter in the cut area or uncut area of the cut sample, or in the uncut samples, there are all no detectable characteristic peaks ($\delta$4.48 and $\delta$5.84) in the spectrum showing activation of *g*DCC. Based on the calculations in the

previous discussion, for the polymer with *g*DCC in the backbones, the minimum amount of mechanophore activation that can increase the energy release correspond to 1 mg of *g*DCC, which is sufficient for the $^{1}$H-NMR detection. For the *g*DCC in the crosslinking positions, the minimum amount also matches 1 mg of the *g*DCC. In this case, if the energy dissipation is higher, the activation of *g*DCC can be detected in the $^{1}$H-NMR spectrum. The results support the conclusion that the stress is not amply transferred to the mechanophores under the testing condition.

# IV. Future Plans

From the temporary results we conclude that there are few activations of *g*DCC mechanophores under tension in the current polymer systems. The first question we need to answer is how to optimize the polymer structure and testing method to more effectively transfer the macroscopic force to the mechanophores in the material. Plans are described as followed,

## *1. Compression Testing*

Compared with the tension test, the compression test is more effective for the stress transfer to activate the mechanophore for the linear *g*DCC-linked polybutadiene.[16] Even though the macroscopic forces that lead to activation are compressive, the individual mechanophore likely experience both tensile and shear forces which cause ring opening. We can translate the compression stress to the tensile stress along the equatorial direction perpendicular to the loading direction as long as the material is of regular shape. It has already been demonstrated that the material will experience higher stress under compression than tension. As shown in the SP incorporated crosslinked PMMA material, the SP in the center of the equatorial plane can experience sufficient stress to undergo ring opening reaction with a distinct color change -- the green intensity increased as the material experienced higher stress.[12] We will explore the relationship between the ultimate transverse stress and strain calculated from the compression data and the activation percentage of *g*DCC. By comparing the result with the tension test, we

can investigate the threshold stress/strain for the activation of the mechanophore in the crosslinked PB system and demonstrate whether the difference in the ultimate stress/strain is the reason for the mechanical silence of the *g*DCC polymer in the monotonic tension test.

## 2. Mechanophore Choice

Our recent work in the SMFS has shown that the force needed to open the *g*DCC ring is higher (*ca.* 1.35 nN) than the *g*DBC ring (*ca.* 1.2 nN) on the same time scale. Based on these results, the *g*DBC mechanophore is more mechanically active than *g*DCC mechanophore. The stability of the *g*DHC mechanophore can be attributed to many factors, including the stereochemical environment, inductive effect of the halogene group, *etc.*[30] The ring opening reaction occurs more readily for *g*DBC than *g*DCC has been attributed to the negative inductive effect of the chlorine, which causes the carbonium ion to be of higher energy than with bromine.[31] As a result, it is reasonable to investigate whether the mechanical activation can be achieved more readily in the crosslinked polymer by replacing the *g*DCC with *g*DBC mechanophore.

## 3. Polymer Matrix Choice

As demonstrated in the SP-PMA and SP-PMMA system,[7,26,12,32] the activation of the mechanophore in the bulk material (tension, compression, torsion) is strain-determined,[28] which means the material needs to pass a threshold strain (in these cases pass the yield strain of the material) to activate the incorporated mechanophores. As

discussed in the discussion section, our system did not show any obvious yield strain prior to polymer failure. If the *g*DCC can be incorporated into PMA or a similar polymer matrix, it is highly possible the mechanophore can be activated, since the activation energy of the SP is higher than that of the *g*DCC mechanophore. A highly *g*DCC-crosslinked PMA is being synthesized and the corresponding mechanical properties will be investigated.

## *4. Colorimetric Indicator/ Luminescent Indicator*

Because of the detection limit of the equipment, so far we have not observed activation of the *g*DCC mechanophore in our system. At this point, it is very helpful to have a secondary mechanophore with a more sensitive macroscopic response that can indicate the stress/strain distribution in the system. SP and/or dioxetane mechanophores are very suitable for this purpose, as they function as colorimetric or luminescent indicators, respectively. By incorporating the secondary mechanophore into the same position (backbone/crosslinker) as *g*DCC, we can monitor whether the macroscopic force is efficiently transferred to the specific position desired by monitoring the color change or light emitted from the activated indicators. Our recent work has shown that by modifying the chemical structure of SP we can incorporate it into the polydimethylsiloxane (PDMS) systems without the loss of the mechanochemical properties. A similar reaction to incorporate the SP into the crosslinking position in the

polybutadiene polymer is under exploration and the mechanical activation behavior will be investigated.

## *5. Supplementary Network*

As briefly mentioned in the discussion section, our system is an organogel consisting of cross-linked macromolecules and solvents. Organogels are typically weak and brittle, and there are two main reasons for this lack in mechanical strength. First is the solution-like nature, *i.e.* low density of polymer chains and small friction between the polymer chains. Another reason is the heterogeneity of the network structure formed during gelation.[33,34,35] The stress is highly localized around the flaws in the material and leads to a failure of the sample at a very low force. One approach to improve the mechanical properties of these gels is introducing another network into the system to form an interpenetrating network (IPN).[36]

Among different IPNs, of particular interest to us is the double network (DN), in which a loosely crosslinked network is incorporated within a swollen heterogeneous polymer network.[37] Essential features of DN gels are as followed: it consists of two kinds of polymers with very different structures. A rigid and brittle polymer serves as the first network, and a soft and ductile polymer serves as the second network. The molar concentration of the second network is 20 to 30 times the first network.[37]

The DN gel is commonly synthesized via a two-step network formation: the first step is forming a tightly crosslinked network. Then the first gel is immersed in the

solution of a second monomer with a low ratio of crosslinkers and process a second polymerization in the first network.[38] The mechanical properties of DN gels were shown to be much better than that of the individual components.[37,38-39] One proposed mechanism for the toughening mechanism is that, when a DN gel under tensile deformation passes a critical stress, the first network fractures to clusters and these clusters behave as a sliding crosslinker of the second network as shown in Figure **16**.

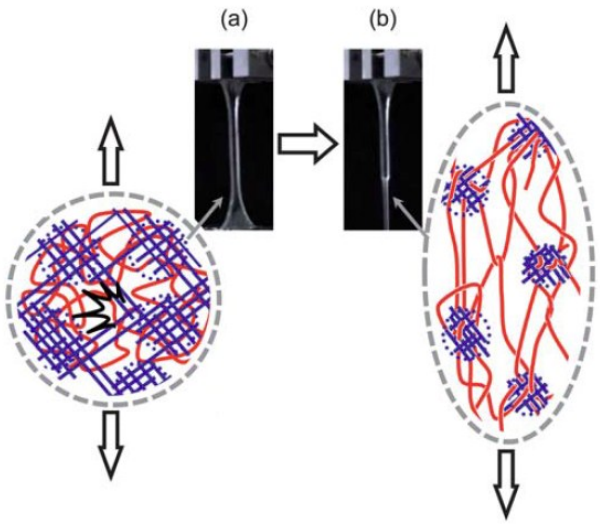


**Figure 16: Illustration of the network structure of a DN gel before (a) and after (b) passing a critical strain.**

Dynamic light scattering (DLS)[39] and small-angle neutron scattering (SANS)[40] studies show that the two networks are tightly coupled and interact favorably with each other, indicating the strong entanglement between the two polymers, which may account for the force transmission from the second network to the first one.

The advantage of introducing a second network into our system to form an IPN or DN network is that during deformation, the failure of the network with relatively poor mechanical properties (first network) will not cause the failure of the whole polymer. Instead, with the support of the other network (second network), the remaining parts of the first network can still be deformed, resulting in a more efficient stress transfer from the second network to the target polymer network. The possible candidates for the second network currently include acrylic copolymer elastomers VHB and polydimethylsiloxane (PDMS), both of which have high ultimate stress and strain. The compatibility between the two networks will be the starting point of this plan.

## *6. Force Induced Crosslinking*

A long term goal to this project is the force induced crosslinking in the bulk towards rational design of self-healing or self-strengthening materials. Mechanoresponsive materials with the ability of self-healing have been actively explored in the past. Conventionally, light or heat is often used to heal the polymer by providing the necessary energy to pass the barrier to create or reform the chemical bonds. Examples include heat-induced reformation of perfluorocyclobutanes,[41]

crosslinked polymeric materials based on Diels-Alder reactions,[42] supramolecular polymer blend based on aromatic pi-pi stacking and hydrogen-bonding interactions,[43] and photo-induced crosslinking of polymers by sulfur-based chain-transfer agents.[44] Despite the inspiring successes, all these healing processes need human intervention, which limits an intrinsic, autonomic response of the material. Autonomic systems where the destructive force can simultaneously activate the healing process are seldom. One approach to the development of the autonomic system is through the mechanochemical transduction that takes advantage of the mechanophore intrinsic property. Under mechanical stimuli, the latent mechanophores can respond in a productive fashion and the damage is mitigated in the meantime, for example by increasing crosslinking density of the material.

Much effort has been made towards the development of the autonomic system in the past. One inspiration is from the ring opening reaction of the *g*DBC mechanophore. Besides the stress relief and the contour length increment, another important result from the reaction is the 2,3-dibromoalkene product which is susceptible to nucleophilic substitution, providing the basis for remodeling and potential self-strengthening or self-repair through covalent cross-linking. Our previous work has shown that under extrusion conditions, a *g*DBC-PB copolymer forms 2,3-dibromoalkenes, and the corresponding allylic bromide can be replaced by chloride through nucleophilic displacement reaction.[18] Recent work has also demonstrated that under extrusion and

sonication condition, *g*DBC-PB copolymer mixed with di-tetrabutylammonium sebatate can be crosslinked through nucleophilic displacement reaction and form gels. For the crosslinked polymers, a *gem*-dichlorocyclopropane mechanophore based on a 1,3-substituted indene was synthesized in Moore group[45] and incorporated in the crosslinked PMA as crosslinkers. Under compression the mechanophore was activated and released hydrochloric acid through elimination. All these results suggest *g*DHC a promising candidate towards the design of the self-healing material through force-induced crosslinking in the material and we will continue exploring this area through rational design of the polymer network with incorporation of optimized functional groups and keep investigating the mechanochemistry in the polymer network.

# V. Experimental Section

## *Material*

**(*Z*)-9,9-dichlorobicyclo[6.1.0]non-4-ene 1a.** (1*Z*,5*Z*)-cycloocta-1,5-diene (127 g, 1180 mmol, 1 eq), chloroform (140.9 g, 1180 mmol, 1 eq) and cetrimonium bromide (CTAB) (50 g, 137 mmol, 0.1 eq, phase transfer catalyst) were dissolved in 600 mL dichloromethane. NaOH solution (472 g, 11.8 mol, 10 eq, in 600 mL deionized water) was added in portions and the mixture was stirred for 1 day under $N_2$ protection. It was subsequently washed with saturated NaCl solution and then concentrated *in vacuo.* Hexane was then used to remove CTAB in the mixture. Pure product was obtained by distilling the mixture under reduced pressure as colorless liquid (191 g, 60%). $^1$H-NMR ($CHCl_3$, 400 MHz): δ 5.55 (dd, 2H) 2.38-2.31 (m, 2H) 2.14-2.02 (m, 4H) 1.88-1.81 (m, 2H) 1.65-1.61 (m, 2H).

**(*Z*)-9-oxabicyclo[6.1.0]non-4-ene 1b.** *m*CPBA (260 g, 1129 mmol, 1 eq) was dissolved in 2000 mL $CHCl_3$ and (1*Z*,5*Z*)-cycloocta-1,5-diene (122 g, 1129 mmol, 1 eq) was dissolved in 200 mL $CHCl_3$. The *m*CPBA solution was added to **1** dropwise using addition funnel over 2 hr. After the mixture was stirred overnight at room temperature, it was washed with 400 mL $NaHSO_3$, 400 mL NaCl, 400 mL $NaHCO_3$ and 400 mL K+Na tartrate. The solution was concentrated *in vacuo*. The crude product was purified by distillation under reduced pressure which afforded the product (68 g, 60%) as colorless

liquid. The b.p. of product is 35~39°C. $^1$H-NMR ($CHCl_3$, 400 MHz): δ 5.54 (m, 2H), 2.99 (m, 2H), 2.40 (m, 2H), 2.10-2.00 (m, 6H).

**(*Z*)-cyclooct-4-enol 1c. 1b** (70 g, 566 mmol, 1 eq), was dissolved in 350 mL anhydrous THF and lithium aluminum hydride (43 g, 1129 mmol, 2 eq) was dissolved in 1050 mL anhydrous THF. **1b** solution was added to the LAH solution dropwise and the mixture was cooled to 0 °C. After stirring under $N_2$ protection for 12 h while allowing the solution to warm up to room temperature, the mixture was quenched with deionized water until no bubbles formed. The mixture was diluted with 1500 mL ethyl ether and washed with 300 mL Deionized water 3 times. Then the solution was concentrated *in vacuo* to provide the product (50 g, 80%). $^1$H-NMR ($CHCl_3$, 400 MHz): δ 5.61 (m, 2H) 3.80 (m, 1H) 2.27 (m, 2H) 2.12(m, 2H) 1.88 (m, 2H) 1.71-1.49 (m, 4H).

**3,3'-(3,3-dichlorocyclopropane-1,2-diyl)dipropanoic acid 1d. 1a** (1 g, 5.2 mmol, 1 eq) and $NaHCO_3$ (0.43 g, 5.2 mmol, 1 eq) were mixed in acetone (15 mL). $KMnO_4$ (2.48 g, 15.7 mmol, 3 eq) was added in small portions to the stirred mixture at room temperature. The mixture was stirred for 2 days. Excess $KMnO_4$ was destroyed by addition of methanol, and the reaction mixture was evaporated to dryness. The residue was treated with water (50 mL) and filtered to remove $MnO_2$. Water layer was acidified with 2N HCl to pH~2 and evaporated to dryness. The remainder was extracted with hot acetone (2 ×25 mL). The solvent was removed under reduced pressure to yield crude product and purified by column chromatography eluting with a mixture of hexane and

ethyl acetate (hexane: ethyl acetate = 1:5; $R_f$ = 0.5). The product (0.67 g, 50%) is a colorless, viscous oil. $^1$H-NMR ($CHCl_3$, 400 MHz): δ 8.51 (b, 2H) 2.53 (m, 4H) 1.77 (m, 4H) 1.66 (m, 2H).

**di((Z)-cyclooct-4-en-1-yl) 3,3'-(3,3-dichlorocyclopropane-1,2-diyl)dipropanoate 2a.** *N,N'*-diisopropylcarbodiimide (DIC) (16 g, 127 mmol, 3 eq) was added to the mixture of **1c** (13 g, 103 mmol, 2.5 eq), **1d** (10.8 g, 42.4 mmol, 1 eq) and 4-dimethylaminopyridine (DMAP) (2.6 g, 21.1 mmol, 0.5 eq) in 200 mL anhydrous THF. After the solution was stirred overnight at room temperature, it was diluted with 1000 mL ethyl ether and washed with deionized water 3 times. The crude product was purified by column chromatography eluting with a mixture of hexane and ethyl acetate (hexane: ethyl acetate = 4:1; $R_f$ = 0.5). The product (2.8 g, 61%) is a colorless, viscous oil. $^1$H-NMR ($CHCl_3$, 400 MHz): δ 5.64 (m, 4H) 4.84 (m, 2H) 2.42-2.18 (m, 10H) 1.86-1.60 (m, 20H).

**di((Z)-cyclooct-4-en-1-yl) glutarate 2b.** DIC (3.6 g, 28.6 mmol, 3 eq) was added to the mixture of **1c** (3 g, 23.8 mmol, 2.5 eq), glutaric acid (1.257 g, 9.5 mmol, 1 eq) and DMAP (0.581 g, 4.8 mmol, 0.5 eq) in 20 mL anhydrous THF. After the solution was stirred overnight at room temperature, it was diluted with 100 mL ethyl ether and washed with deionized water 3 times. The crude product was purified by column chromatography eluting with a mixture of hexane and ethyl acetate (hexane: ethyl acetate = 9:1; $R_f$ = 0.45). The product (1.32 g, 40%) is a colorless, viscous oil. $^1$H-NMR

($CHCl_3$, 400 MHz): δ 5.64 (m, 4H) 4.80 (m, 2H) 2.23 (m, 6H) 2.13 (m, 8H) 1.85 (m, 8H) 1.67 (m, 4H).

**di((Z)-cyclooct-4-en-1-yl) octanedioate 2c.** DIC (19.44 g, 154 mmol, 3 eq) was added to the mixture of **1c** (16.2 g, 128 mmol, 2.5 eq), octanedioic acid (8.95 mg, 51.4 mmol, 1 eq) and DMAP (3.14 g, 25.7 mmol, 0.5 eq) in 200 mL anhydrous THF. After the solution was stirred overnight at room temperature, it was diluted with 1000 mL ethyl ether and washed with D.I. water 3 times. The solution was concentrated *in vacuo* to give the crude product. The crude product was purified by column chromatography eluting with a mixture of hexane and ethyl acetate (hexane: ethyl acetate = 8:1; $R_f$ = 0.5). The product (13.8 g, 69%) is a colorless, viscous oil. $^1$H-NMR ($CHCl_3$, 400 MHz): δ 5.66 (m, 4H) 4.82 (m, 2H) 2.24-2.14 (m, 12H) 1.86-1.60 (m, 12H) 1.32 (m, 4H).

**Backbone *g*DCC-functionalized crosslinked polybutadiene 3a to 3e.** The crosslinked polybutadiene polymer with *g*DCC embedded was synthesized through ROMP reaction with different ratios of (1*Z*,5*Z*)-cycloocta-1,5-diene (eq: 100, 80 50, 20, 0), **1a** (eq: 0, 20, 50, 80, 100) and **2b** (eq: 4) with 2,6-bis(1,1-dimethylethyl)-4-methylphenol (BHT) (0.1wt%) as the stabilizer. All starting materials were added stoichiometrically to a 7 mL vial and kept in the cold room at 4 ℃ for 1 h. To the mixture was then added 2$^{nd}$ generation Grubbs catalyst (eq: 0.1) in 1,2-dichloroethane (0.25g/mL). The mixture was poured into a PTFE mold covered with glass and aluminum foil, and subsequently cast in the oven at 70 ℃ for 3 h, and then dried under high vacuum for 12 h. The polymers

are dark yellow, homogeneous, transparent, thin films with thickness between 0.40 and 0.80mm.

**Crosslinker *g*DCC-functionalized crosslinked polybutadiene 4a. 4a** was synthesized through ROMP reaction with molar ratio of 100 to 4 between (1Z,5Z)-cycloocta-1,5-diene and **2a**. Starting materials were added stoichiometrically ((1Z,5Z)-cycloocta-1,5-diene 2500 mg, 23.15 mmol, 100 eq; **2a** 433.78 mg, 0.926 mmol, 4 eq; BHT 2.9 mg, 0.1wt%) to a 7 mL vial and kept in the cold room at 4 °C for 1 h. To the mixture was then added 2nd generation Grubbs catalyst (20 mg, 0.023 mmol, 0.1 eq) in 1,2-dichloroethane (80 μL). The mixture was poured into a PTFE mold covered with glass and aluminum foil, and subsequently cast in the oven at 70 ℃ for 3 h to give the product. The crosslinked polymer was then dried under high vacuum for 12 h. The polymer is a dark yellow, homogeneous, transparent, thin film with a thickness between 0.50 and 0.60mm.

**Crosslinker *g*DCC-functionalized crosslinked polybutadiene 4c. 4c** was synthesized through ROMP reaction with ratio of 100 to 1 between **1a** and **2a**. Starting materials were added stoichiometrically (**1a** 3500 mg, 18.32 mmol, 100 eq; **2a** 77.0 mg, 0.16 mmol, 1 eq; BHT 3.6 mg, 0.1 wt%) to a 7 mL vial and kept in the cold room at 4 °C for 1 h. To the mixture was then added 2nd generation Grubbs catalyst (15.6 mg, 0.018 mmol, 0.1 eq) in 1,2-dichloroethane (63 μL). The mixture was poured into a PTFE mold covered with glass and aluminum foil, and subsequently cast in the oven at 70 °C for 3 h

to give the product. The crosslinked polymer was then dried under high vacuum for 12 h. The polymer is a dark yellow, homogeneous, transparent, thin film with a thickness between 0.50 and 0.70 mm.

**Control Crosslinked polybutadiene 4b. 4b** was synthesized through ROMP reaction with ratio of 100 to 4 between (1*Z*,5*Z*)-cycloocta-1,5-diene and **2c**. Starting materials were added stoichiometrically ((1*Z*,5*Z*)-cycloocta-1,5-diene 2500 mg, 23.15 mmol, 100 eq; **2c** 359.4 mg, 0.926 mmol, 4 eq; BHT 2.8 mg, 0.1wt%) to a 7 mL vial and kept in the cold room at 4 $^{o}$C for 1 h. To the mixture was then added 2$^{nd}$ generation Grubbs catalyst (20 mg, 0.023 mmol, 0.1 eq) in 1,2-dichloroethane (80 μL). The mixture was poured into a PTFE mold covered with glass and aluminum foil, and subsequently cast in the oven at 70 $^{o}$C for 3 h to give the product. The crosslinked polymer was then dried under high vacuum for 12 h. The polymer is a dark yellow, homogeneous, transparent, thin film with a thickness between 0.50 and 0.70mm.

**Control Crosslinked polybutadiene 4d**. **4d** was synthesized through ROMP reaction with ratio of 100 to 1 between **1a** and **2c**. Starting materials were added stoichiometrically (**1a** 3500 mg, 18.32 mmol, 100 eq; **2c** 63.8 mg, 0.16 mmol, 1 eq; BHT, 0.1 wt%) to a 7 mL vial and kept in the cold room at 4 $^{o}$C for 1 h. To the mixture was then added 2$^{nd}$ generation Grubbs catalyst (15.6 mg, 0.018 mmol, 0.1 eq) in 1,2-dichloroethane (63 μL). The mixture was poured into a PTFE mold covered with glass and aluminum foil, and subsequently cast in the oven at 70 $^{o}$C for 3 h to give the product. The

crosslinked polymer was then dried under high vacuum for 12 h. The polymer is a dark yellow, homogeneous, transparent, thin film with a thickness between 0.40 and 0.80 mm.

# References


1. Launey, M. E.; Ritchie, R. O., On the Fracture Toughness of Advanced Materials. *Adv Mater* **2009,** *21* (20), 2103-2110.

2. Caruso, M. M.; Davis, D. A.; Shen, Q.; Odom, S. A.; Sottos, N. R.; White, S. R.; Moore, J. S., Mechanically-Induced Chemical Changes in Polymeric Materials. *Chem Rev* **2009,** *109* (11), 5755-5798.

3. Kauzmann, W.; Eyring, H., The Viscous Flow of Large Molecules. *J Am Chem Soc* **1940,** *62*, 3113-3125.

4. Bell, G. I., Theoretical-Models for the Specific Adhesion of Cells to Cells or to Surfaces. *Adv Appl Probab* **1980,** *12* (3), 566-567.

5. Encina, M. V.; Lissi, E.; Sarasua, M.; Gargallo, L.; Radic, D., Ultrasonic Degradation of Polyvinylpyrrolidone - Effect of Peroxide Linkages. *J Polym Sci Pol Lett* **1980,** *18* (12), 757-760.

6. Hickenboth, C. R.; Moore, J. S.; White, S. R.; Sottos, N. R.; Baudry, J.; Wilson, S. R., Biasing Reaction Pathways with Mechanical Force. *Nature* **2007,** *446* (7134), 423-427.

7. Beiermann, B. A.; Davis, D. A.; Kramer, S. L. B.; Moore, J. S.; Sottos, N. R.; White, S. R., Environmental Effects on Mechanochemical Activation of Spiropyran in Linear PMMA. *J Mater Chem* **2011,** *21* (23), 8443-8447.

8. Cho, S. Y.; Kim, J. G.; Chung, C. M., A Fluorescent Crack Sensor Based on Cyclobutane-containing Crosslinked Polymers of Tricinnamates. *Sensor Actuat B-Chem* **2008,** *134* (2), 822-825.

9. Chen, X. X.; Wudl, F.; Mal, A. K.; Shen, H. B.; Nutt, S. R., New Thermally Remendable Highly Cross-linked Polymeric Materials. *Macromolecules* **2003,** *36* (6), 1802-1807.

10. Szalai, M. L.; McGrath, D. V.; Wheeler, D. R.; Zifer, T.; McElhanon, J. R., Dendrimers based on Thermally Reversible Furan-maleimide Diels-Alder Adducts. *Macromolecules* **2007,** *40* (4), 818-823.

11. Chung, C. M.; Roh, Y. S.; Cho, S. Y.; Kim, J. G., Crack Healing in Polymeric Materials via Photochemical [2+2] Cycloaddition. *Chem Mater* **2004,** *16* (21), 3982-+.

12. Davis, D. A.; Hamilton, A.; Yang, J. L.; Cremar, L. D.; Van Gough, D.; Potisek, S. L.; Ong, M. T.; Braun, P. V.; Martinez, T. J.; White, S. R.; Moore, J. S.; Sottos, N. R., Force-induced Activation of Covalent Bonds in Mechanoresponsive Polymeric Materials. *Nature* **2009,** *459* (7243), 68-72.

13. Chen, Y. L.; Spiering, A. J. H.; Karthikeyan, S.; Peters, G. W. M.; Meijer, E. W.; Sijbesma, R. P., Mechanically Induced Chemiluminescence from Polymers Incorporating a 1,2-Dioxetane Unit in the Main Chain. *Nat Chem* **2012,** *4* (7), 559-562.

14. Wu, D.; Lenhardt, J. M.; Black, A. L.; Akhremitchev, B. B.; Craig, S. L., Molecular Stress Relief through a Force-Induced Irreversible Extension in Polymer Contour Length. *J Am Chem Soc* **2010,** *132* (45), 15936-15938.

15. Klukovich, H. M.; Kouznetsova, T. B.; Kean, Z. S.; Lenhardt, J. M.; Craig, S. L., a Backbone Lever-arm Effect Enhances Polymer Mechanochemistry. *Nat Chem* **2013,** *5* (2), 110-114.

16. Lenhardt, J. M.; Black, A. L.; Beiermann, B. A.; Steinberg, B. D.; Rahman, F.; Samborski, T.; Elsakr, J.; Moore, J. S.; Sottos, N. R.; Craig, S. L., Characterizing the Mechanochemically Active Domains in gem-Dihalocyclopropanated Polybutadiene under Compression and Tension. *J Mater Chem* **2011,** *21* (23), 8454-8459.

17. Lenhardt, J. M.; Black, A. L.; Craig, S. L., gem-Dichlorocyclopropanes as Abundant and Efficient Mechanophores in Polybutadiene Copolymers under Mechanical Stress. *J Am Chem Soc* **2009,** *131* (31), 10818-+.

18. Black, A. L.; Orlicki, J. A.; Craig, S. L., Mechanochemically Triggered Bond Formation in Solid-state Polymers. *J Mater Chem* **2011,** *21* (23), 8460-8465.

19. Akbulatov, S.; Tian, Y. C.; Boulatov, R., Force-Reactivity Property of a Single Monomer is Sufficient to Predict the Micromechanical Behavior of its Polymer. *J Am Chem Soc* **2012,** *134* (18), 7620-7623.

20. Neises, B.; Steglich, W., Simple Method for the Esterification of Carboxylic Acids. *Angew Chem Int Edit* **1978,** *17*, 522-524.

21. Bandari, R.; Prager-Duschke, A.; Kuhnel, C.; Decker, U.; Schlemmer, B.; Buchmeiser, M. R., Tailored Ring-opening Metathesis Polymerization Derived Monolithic Media Prepared from Cyclooctene-based Monomers and Cross-linkers. *Macromolecules* **2006,** *39* (16), 5222-5229.

22. Lake, G. J.; Thomas, A. G., The Strength of Highly Elastic Materials. *Proc R Soc Lon Ser-A* **1967,** *300* (1460), 108-119.

23. Rivlin, R. S.; Thomas, A. G., Rupture of Rubber .1. Characteristic Energy for Tearing. *J Polym Sci* **1953,** *10* (3), 291-318.

24. Irwin, G. R., Fracture. *handbuch der physik* **1958,** *6*, 551-590.

25. Abdel-Magid, A. F.; Cohen, J. H.; Maryanoff, C. A.; Shah, R. D.; Villani, F. J.; Zhang, F., Hydrolysis of Polypeptide Esters with Tetrabutylammonium Hydroxide. *Tetrahedron Lett* **1998,** *39* (21), 3391-3394.

26. Kingsbury, C. M.; May, P. A.; Davis, D. A.; White, S. R.; Moore, J. S.; Sottos, N. R., Shear Activation of Mechanophore-crosslinked Polymers. *J Mater Chem* **2011,** *21* (23), 8381-8388.

27. Flory, P. J., *Principles of Polymer Chemistry*. Cornell University Press: Ithaca,, 1953; p 672 p.

28. Eyring, H., Viscosity, Plasticity, and Diffusion as Examples of Absolute Reaction Rates. *J Chem Phys* **1936,** *4* (4), 283-291.

29. Gorner, H., Photochromism of Nitrospiropyrans: Effects of Structure, Solvent and Temperature. *Phys Chem Chem Phys* **2001,** *3* (3), 416-423.

30. Baird, M. S.; Reese, C. B., Action of Heat on Halogenocarbene Adducts of Cycloheptene and Cis-Cyclo-Octene. *J Chem Soc C* **1969,** (13), 1803-&.

31. Baird, M. S., Lindsay, D. G., Reese, C. B., Thermal Rearrangement of Halogenocarbene Adducts of Cyclic Olefins. *J Chem Soc C* **1969,** (8), 1173-1178.

32. Lee, C. K.; Davis, D. A.; White, S. R.; Moore, J. S.; Sottos, N. R.; Braun, P. V., Force-Induced Redistribution of a Chemical Equilibrium. *J Am Chem Soc* **2010,** *132* (45), 16107-16111.

33. Tanaka, T.; Sato, E.; Hirokawa, Y.; Hirotsu, S.; Peetermans, J., Critical Kinetics of Volume Phase-Transition of Gels. *Phys Rev Lett* **1985,** *55* (22), 2455-2458.

34. Osada, Y.; Okuzaki, H.; Hori, H., A Polymer Gel with Electrically Driven Motility. *Nature* **1992,** *355* (6357), 242-244.

35. Yoshida, R.; Uchida, K.; Kaneko, Y.; Sakai, K.; Kikuchi, A.; Sakurai, Y.; Okano, T., Comb-Type Grafted Hydrogels with Rapid De-Swelling Response to Temperature-Changes. *Nature* **1995,** *374* (6519), 240-242.

36. Sperling, L. H.; Mishra, V., The Current Status of Interpenetrating Polymer Networks. *Polym Advan Technol* **1996,** *7* (4), 197-208.

37. Gong, J. P., Why are Double Network Hydrogels so Tough? *Soft Matter* **2010,** *6* (12), 2583-2590.

38. Gong, J. P.; Katsuyama, Y.; Kurokawa, T.; Osada, Y., Double-network Hydrogels with Extremely High Mechanical Strength. *Adv Mater* **2003,** *15* (14), 1155-+.

39. Huang, M.; Furukawa, H.; Tanaka, Y.; Nakajima, T.; Osada, Y.; Gong, J. P., Importance of Entanglement between First and Second Components in High-strength Double Network Gels. *Macromolecules* **2007,** *40* (18), 6658-6664.

40. Tominaga, T.; Tirumala, V. R.; Lee, S.; Lin, E. K.; Gong, J. P.; Wu, W. L., Thermodynamic Interactions in Double-network Hydrogels. *J Phys Chem B* **2008,** *112* (13), 3903-3909.

41. Klukovich, H. M.; Kean, Z. S.; Iacono, S. T.; Craig, S. L., Mechanically Induced Scission and Subsequent Thermal Remending of Perfluorocyclobutane Polymers. *J Am Chem Soc* **2011,** *133* (44), 17882-17888.

42. Chen, X. X.; Dam, M. A.; Ono, K.; Mal, A.; Shen, H. B.; Nutt, S. R.; Sheran, K.; Wudl, F., A Thermally Re-mendable Cross-linked Polymeric Material. *Science* **2002,** *295* (5560), 1698-1702.

43. Burattini, S.; Greenland, B. W.; Merino, D. H.; Weng, W. G.; Seppala, J.; Colquhoun, H. M.; Hayes, W.; Mackay, M. E.; Hamley, I. W.; Rowan, S. J., A Healable Supramolecular Polymer Blend Based on Aromatic pi-pi Stacking and Hydrogen-Bonding Interactions. *J Am Chem Soc* **2010,** *132* (34), 12051-12058.

44. Scott, T. F.; Schneider, A. D.; Cook, W. D.; Bowman, C. N., Photoinduced Plasticity in Cross-linked Polymers. *Science* **2005,** *308* (5728), 1615-1617.

45. Diesendruck, C. S., B.; Sugai, N.; Silberstein, M.; Sottos, N.; White, S.; Braun, P.; Moore, J., Proton-Coupled Mechanochemical Transduction: A Mechanogenerated Acid. *J Am Ceram Soc* **2012,** *134* (30), 12446-12449.